JOINT EUROPEAN TORUS

JET–P(92)81

J. Wade, J. Jacquinot, G. Bosia, A. Sibley, M. Schmid
and JET Team

Development of the JET ICRH Plant

Development of the JET ICRH Plant

T.J. Wade, J. Jacquinot, G. Bosia, A. Sibley, M. Schmid
and JET Team*

JET-Joint Undertaking, Culham Science Centre, OX14 3DB, Abingdon, UK

** See Annex*

Preprint of Paper to be submitted for publication in
Fusion Engineering

ABSTRACT.

The JET 32MW ICRF system Is modular In construction and consists of eight Independent generator-antenna units operating at frequencies In the range 23–7MHz. The system Is controlled remotely, and all real time functions, such as the matching to the plasma load, are performed automatically during the tokamak pulse. The flexibility and versatility of the plant have successfully permitted a continuing development programme since the system commenced operation In 1985.

The total power of the eight generators has been upgraded from 24 to 32MW, of which over 22MW has been coupled Into the plasma centre. The plant and power availability has been considerably improved by enhancing the automatic matching and protection circuitry. The operating regimes have been extended beyond the original conceptual design, making It possible to heat during "L" to "H" mode transitions and perform preliminary Fast Wave Current Drive experiments. New facilities will enable phased conductor FWCD experiments with the four-element (A2) antenna arrays during the pumped dlvertor phase of JET.

This paper reviews the enhancements to the plant since Its Inception, especially to the control circuitry, which have resulted from analysts and understanding of the fast varying antenna-plasma load and from operating under Increasingly more stringent conditions. References to the associated ICRH physics are given. The developments of the JET antennae are described In the companion paper "Present and Future JET ICRH Antenna" by A S. Kaye.

Introduction and System Architecture

The JET ICRF system was conceived with a modular construction, to be operated remotely from the JET Control Room, and with all essential functions, such as matching the generators to the plasma load, performed automatically on line during the tokamak pulse. Flexibility and versatility successfully built into the plant from its inception permits a continuing development programme for the plant and its control functions in line with the physics requirements described in [1], [2]. The development of the JET antennas is described in [3].

A generator plant producing 30 MW of RF power was originally specified [4] to provide 15MW of ICRF heating at the centre of the JET plasma whilst allowing for transmission and coupling losses in the worst case. The size and number of generator modules forming the ICRH plant were determined by two factors, (i) the unit power output of 1.5-2 MW from available RF tetrodes over the JET ICRH frequency range of 23 - 57 MHz, and (ii) the power handling of the coaxial feeds to the antennas through the limiter guide tubes already built into JET. Encouraging initial results [5], resulted in an upgraded plant specification of 8 x 4 MW Generator-antenna units [6].

The present JET ICRH system consists of eight tandem generator- antenna units, the main characteristics of which are summarized in table 1. The 8 installed generators are shown in Fig. (1). Each of the eight RF generators consists of two 2MW amplifiers and feeds one antenna through two 30 ohm 84 m long 230 mm dia transmission lines, an example of which can be seen in the foreground. A schematic of one generator unit is shown in Fig. 2. At the generator end of the transmission line there is a 3 m tuning stub, and a trombone phase shifter to equalize the line electrical length. For some of the operating periods an additional capacitive stub was fitted near the antenna [7]. Each Generator-antenna transmission line has been engineered to the same length (84m) to give identical matching control characteristics and to permit phased arrays with single frequency operation. The generator modules and their DC supplies are completely independent except for two facilities. The incoming 33kV HV AC circuit breakers and some aspects of the tetrode anode demineralised water cooling systems are shared between two generator modules. This modularity permits the requirements of the physics programme to be met even during plant component failures. For example the maximum power capability is only reduced by 1/8 or 12% during a tetrode replacement.

The ICRH plant is remotely operated requiring no separate local control desk, no personnel at the plant itself, and only one or two staff in the JET control room. Parameters such as power output, operating frequency and starting settings are stored and loaded by the computer, whilst matching is performed automatically by various nested feedback loops during the pulse. Operating frequency changes requested by the physics programme are performed between plasma pulses and take about 1 minute. The full 8 antenna system has been operational since mid 1987, and the generator upgrade to 4 MW was completed at the end of 1989.

This paper is divided into three sections. Section (1) describes the increased power availability from the amplifier chain and the tetrode output circuit for plasma heating. Section (2) describes the parameters of the control and protection system operational until 1992 and includes the automatic matching system and plasma position control. Section (3) describes the ICRF plant upgrade for the pumped divertor phase of JET and includes the new facilities for Fast Wave Current Drive. Practical operational experience of ICRH at JET until 1992 has been described in [8].

1.0 Amplifier enhanced power availability

1.1 *Amplifier chain description.*

A JET ICRH plant single 2 MW amplifier chain is shown schematically as part of the control block diagram (Fig. 3) and has been described in detail in [9].

A phase and amplitude modulated 1 mW frequency source drives a 600 watt solid state wideband amplifier, which in turn drives 3 tuned tetrode stages operating at the nominal powers shown. With amplitude feedback the amplifier chain has the required wide bandwidth of 4 MHz, specified to allow coverage of the operating frequency range of 23-57 MHz in 8 steps or "channels". The number of tuning elements required to change

frequency has been reduced to a minimum of 11 for the three stages including the output transformer. As a result the static bandwidth is narrower and the preamplifier and driver tetrodes are overated to compensate for the resultant loss of gain at the band edges. Automatic tuning circuits were not found necessary, but a resulting additional power limiter to "clip" the reserve capacity of drive stages was needed and is described in the next section.

To obtain the maximum output power into varying loads over the 23-57 MHz range the 2 MW output tetrode is operated as a grounded (control) grid amplifier, with a DC grounded screen grid nominally in class "B" (180^{o} RF conduction angle). See Fig. 4. Routine DC to RF conversion at the anode of 75% is achieved, close to the class "B" theoretical figure of 78%. Specific tests with fine adjustment of the bias voltages and the tuning have achieved efficiencies of 82% at 43MHz and 84% at 25MHz. In this case the tube is operating just into class "C". The total plant operates at an efficiency of 65% conversion of DC plus auxillary power input to RF power out. A full discussion of the merits of various tube operating scenarios appears in earlier literature [10][11][12]. Development of more efficient tubes for longer pulse or even steady state operation also continues [13]. The original JET ICRH HVDC supplies are described in [14]. Tables 1 & 3 show their present upgraded capability.

1.2 Maximum power improvement

As specified in the original design, the JET ICRH generators, transmission lines and antenna are protected against arcs or discharges occurring during operations by detecting these as a high values of reflected RF power at the generator. The RF power is suppressed (tripped) for a few millisecs to allow the ionisation to clear, then power reapplied. In Fig. (5), (a) shows the reflection coefficient "ρ" trip level threshold. The trip is not active at low power levels to allow matching to take place. The trip is faster and always operates before the reflected power limits Fig. (5) (b) even at higher powers (see table 3). Future improvements and additional end stage arc protection using these trip circuits are described later in this paper.

Random events such as the antenna arcs are part of JET operation and contribute to the conditioning of the RF vacuum components. So, with conditioning, the maximum rated voltages of the line and antenna should be obtainable, even if some tripping takes place during a pulse. However, statistical analysis of early JET pulse data showed that the maximum power that was being obtained with the ICRH RF plant per generator was being restricted, and, at the onset of "tripping", was dependent on the transmission line forward voltage before arcing and not the peak voltage rating of the line as explained below.

Fig (6) shows a typical plot of all individual generator power outputs versus coupling resistance, using 1988 data, at an often used operating frequency of 42 MHz. The data has been "filtered" to include only pulses at the limit of power where one or more trip due to arcing has occurred.

Plotted on the same axes, a peak voltage limit Vmax of 25 kV on the transmission line or antenna before arcing is shown by line (a).
The power is given by

$$P = \frac{(V\,max)^2 \,.\, Rc}{2.Zo^2}.$$

Rc = coupling resistance, Zo = characteristic impedance of the line.

A closer model of the limit is given by curve (b), which shows a transmission line forward voltage Vf of 14kV before the arcing
Where the power

$$P = \frac{((1+\rho)Vf)^2 \,.\, Rc}{2.Zo^2}.$$

ρ, the reflection coefficient on the transmission line is a function of Rc, so P simplifies as

$$P = \frac{2.Vf^2 \,.\, Rc}{(Zo+Rc)^2}.$$

Curve (c) is a flat limit related inter-antenna cross-talk discussed later.

To understand the significance of these limits a simplified network shown in Fig. 7 is used to model one ICRH amplifier feeding one half antenna (connection a). The output tetrode anode drives a matching transformer, comprising strip

line inductors and a capacitor, from a nominal anode impedance of 90 ohms to the transmission line Zo of 30 ohms. Fig. 8 shows the output circuit components L2, C3 and L3 with L1, C2 and the tetrode partially visible on the left of the picture. Before the tuning stub, there are approximately 6.5 metres of line containing the measurement and control directional couplers which amongst their other functions operate the generator reflected power trip circuits (in 100 μs). The antenna is connected via 84 metres of virtually lossless line, approx 1.6×10^{-3} dB per metre. Table 2 shows the parameters used in this model (Fig. 7).

Using the model of this composite circuit, the antenna load impedance Rc was replaced with an "arc" or short circuit, derived in table 4, but the tetrode anode current was kept constant, which is valid in the short timescale of an arc (<2 μs). The voltages on the tetrode anode, the central capacitor, and the output inductor in the generator were calculated for all frequencies and coupling resistances (stub settings), to find the worst case when the position of the arc is also varied +/- $\lambda/8$ of a voltage maximum on the transmission line. A typical output result is shown in Fig. 9. Over the range of operating frequencies, the voltage on the tetrode output circuit components (Fig. 7) shown as (+) on the anode A, (o) on the capacitor C, and (•) on the output line L, could far exceed their design ratings, especially where the 6.5 m transmission line causes the maximum impedance transformation at ~35 MHz, and was sufficient to cause "secondary" arcing, explaining some generator damage during operation as described [8].

The maximum power available therefore is related to the operating anode current at the time of arcing, because this must not cause voltages in excess of the maximum rating on the generator components after the antenna arc. Once an antenna arc is established, the voltages on all parts of the network including the transmission line are proportional to that anode current.

Inserting voltage ratings of components in the mathematical model predicts an "envelope" of maximum values of transmission line forward voltage shown in Fig. 10 that compares reasonably accurately with the statistical data for all generators and frequencies from the 1990 period, considering that the model treats the inductors and capacitors as ideal lumped circuit elements whereas in reality their electrical length is not insignificant, see Fig. 8. The same trip data "filter" is applied as in Fig. 5.

1.3 Practical verification of the calculated power restriction

To verify the theoretical predictions of the power restricting mechanism described above, a simulation of a plasma loaded antenna was required such that full power and full line voltage were present at the same time. Previous tests on a short circuited long line (b) in Fig. 8 only require some 200 kW of generator power, a nominal 20 amps tetrode RF current, to produce voltages of 30 kV on the line and do not permit full voltage and power to be tested simultaneously. Plasma loads are not generally available in a controlled manner for generator experiments.

The normal wideband or frequency insensitive test load for a generator does not operate at full line voltage when at full power and therefore would not transform into the "undesirable" impedance for the above limiting effect, if caused to arc. Instead a special tuned load was constructed which comprised a long line terminated in a partial or lossy mismatch formed by an additional stub plus a test load to represent a plasma load, correction (c) in Fig. 8. Setting the equivalent coupling resistance to 4 ohms means that a line voltage of 30 kV is reached with 2 MW from the tetrode, ie with a peak tetrode anode RF current of some 200 amps.

As predicted it was possible with this test rig to provoke inextinguishable arcs in the generator at the capacitor by inducing "test" arcs on the transmission line. Thus following these investigation and tests, additional arc protection and trip circuits were installed in the generator output circuits, eliminating the catastrophic failures experienced earlier and making the generators available for full length pulses up to the full power rating of the components.

22.5 MW of ICRF heating has been achieved at the plasma centre from 26.3 MW total output from the generators. Fig. 10 shows a JET high power pulse and illustrates the trips and arc protection in action. The ragged power envelope is due

to arcing in the end stage of generator 2B and conditioning of antenna 4B, both shown overlaid at the botttom of the figure. (The generator numbering refers to the JET octant and sector.) The endstage ultraviolet arc detectors require a 20ms trip period, and the improved power recovery is obtained with a 1%/ ms voltage slope (100 ms to full power), shown in the 2B trace. Antenna 4B trip circuit was not modified at that time and shows the original shorter 5 ms trips period with approx 2 ms recovery time (see also table 3 in section 2).

1.4 Summary of section 1

High power ICRH (22.5 MW) has been achieved at the plasma centre after modifications and improvements to the amplifiers and their protection system. The "secondary" arc mechanism causing power limitations and generator damage was not forseen at the design stage of the JET ICRH plant. The network of any future ICRF plant should be analysed using model calculations for the effects of arcs as described here and also for the effects of harmonics and transients. The model described above is limited to a steady state fundamental frequency and treats the inductors as lumped elements. Modifying or switching the generator-to-stub 6.5 m transmission line length in the JET plant would remove the remaining power constraint due to this mechanism at certain frequencies around 35 MHz and may be considered in the future.

2.0 The Present ICRH Control and Protection System.

2.1
The ICRH control loops and protection systems most relevant to plasma operation upto 1992 are shown in the overall schematic of one JET amplifier chain, Fig. 3. Modifications and enhancements to the control systems for the divertor phase of JET are described later in Section 3.

The diagram Fig. 3 shows a frequency source feeding the phase and amplitude modulators followed by the 2 MW amplifier chain with a transformer output. This generator output feeds a section of "matched" transmission line with measurement directional couplers, the tuning stub, and the unmatched line to the antenna, which is also equiped with measurment directional couplers. The length of the unmatched line to the antenna can be trimmed by a trombone phase shifter or line stretcher. Most of the protection is part of the original conceptual design of the JET ICRH plant. As can be seen from the diagram, the RF directional couplers are essential in that they provide most of the control and protection functions, except for the basic tube parameters.

The controls are divided into 5 catagories:-

1) Terminate the Pulse,
2) Power Trips,
3) Limits,
4) Requested Values,
5) Automatic Functions.

These are shown in table 3, and each category is grouped together in Fig. 3. Items marked * are added developments.

The differential trip circuit in category (1) operated if the difference in reflection coefficients of the two generator feeds to one antenna exceeded 0.5, the asymmetry thus showing a non plasma related mismatch on one line. If 255 trips occurred the pulse was terminated. However as described in [8] an unwanted discharge simultaneously on both feeds in one antenna was not detected by this system, the power was too low for the trip protection set and damage to that antenna feedthroughs resulted. The differential trip was also vulnerable to the cross-talk described below, and is therefore not being included in the upgraded control system (section 3).

The control grid current limiter in category (3) was added because the reserve capabilities of the drive chain mentioned above in section (1) were not being clipped by tetrode saturation. Instead, on control and load transients such as are trips, the output tetrode control grid was being over driven causing the grid bias supply to trip on overcurrent and terminate the pulse. Initially this additional control grid current limiter was in the form of a drive power limiter set to 100 kW, but this was too conservative under certain load conditions, restricting the power unnecessarily, and was revised to operate directly on the grid current.

The items shown in italics are proposals for the control upgrade (described in section 3) . The two limiters marked **, generator transmission line forward and

reflected power, act as safety backups to the more direct tube parameter limiters.

2.2 *The JET automatic matching System*

To obtain matched loads for the ICRH generators, the JET system uses one parallel motorised tuning stub per transmission line near to the generator, combined with electrical length adjustment of the long (84 m) line feeding the antenna (Fig. 2). A frequency change Δf of 1.78 MHz produces one complete rotation (2π) of the antenna load y(a) reflection coefficient angle $\rho(a)$ at the stub. For the range of plasma loads experienced on JET, only a small frequency change ($\leq$100 kHz) is neccesary therefore to adjust the complex admittance

$$y(a) = g+jb,$$

so that g becomes equal y(o) (the line characteristic admittance), and jb can be cancelled by an inductive shunt tuning stub susceptance (-jb), thus giving a match. This system was first described in [15] [16]. Over the antenna load range, angle (ρ) and jb are nearly orthogonal, permitting the automatic control of these functions by two independent feedback loops to obtain a match for the generator. Furthermore the response of the frequency control loop is rapid, typically <1ms.

Fig. (12) shows a block diagram of the automatic matching control system. The 2 MW generator output transmission line to the shunt tuning stub and the unmatched main transmission line feeding the antenna are fitted with measurement directional couplers. The other functions on the diagram are concerned with antenna current control and are described in section 3. The ratio of the waves travelling away from the stub, the generator output line reflected wave (Vro), and the main transmission line forward wave (Vfm) give a control function:-

$$\sigma = \frac{Vro}{Vfm}$$

where Vro, Vfm, σ, are all vector (complex) quantities.

It has been shown in [15] that the real part

$$re(\sigma) = 0$$

when Vro $\rightarrow$ 0, ie a match, and thus the electrical length which is equivalent to angle $\rho(a)$ is correct.

Also at this value, the imaginary part

$$imag(\sigma) = 0$$

when the stub susceptance = jb the imaginary part of y(a).

Fig. 13 shows a modelled plot of the generator match $\rho(g)$ versus frequency for three stub settings (+/-0.1 m about the match), where the associated control function $re(\sigma) = 0$ when ρg for each trace is a minimum. The re (σ) traces run nearly vertically.

Fig. 14 shows the equivalent match ρg versus stub length for 3 values of frequency
(+/- 100 KHz about the match). Note that the control function imag (σ) (nearly vertical traces) is only correct in both sign and slope for the central (matching) frequency. In practice this problem is overcome by the fast response time of the frequency control loop which achieves ρ minimum (the optimum electrical length) before the stubs have reacted.

The main transmission lines are also equipped with 500 mm motorised "trombone" phase shifters, which also adjust the electrical length. Primarily installed to equalise all the line lengths, these also can be operated by the feedback loop,

i) when the two lines to one antenna are not balanced and require trimming and

ii) when more than one generator is operating phased locked to the same frequency. They are also used when the antenna current phasing is being varied see section (3).

The JET automatic matching system can be used to obtain a match during a power shot even if the plasma coupling is unknown beforehand. Fig. (15) shows a typical operation.
Starting with a reflection coefficient of 0.4 (plot b), a match is obtained in about 2 secs, shown by the stub error signal (d), governed only by the tracking speed of the stubs. Note that the plasma coupling (c) progresses from 3 ohms to 6 ohms with an accompanying frequency shift (e) related to the plasma reactance, during the shot.

2.3 *Coupling resistance control of plasma position*

A novel control system has been installed at JET which enhances the performance of the ICRH on non-limiter plasmas. RF heating can be applied during fast plasma variations such as "L to H" mode transitions, by moving the plasma whose response time (100 ms) is faster that the tuning stubs, to hold the coupling constant.

The Coupling Resistance Control of Plasma Position works in combination with the frequency feedback system described above. It adjusts the plasma position until Rc, the real part of the complex load, corresponds to the requested value. The frequency feedback corrects the imaginary or reactive part of the load to provide a perfect match for the RF generator. The tuning stubs, also in feedback mode but slower to move than the plasma, use a phase derived error signal to correct the real part, and thus correct for the divergence of the individual antenna loads from the mean value.

Fig. 15 shows a typical shot where RF heating is applied across a "L" to "H" mode transition. During the "H" mode (b) the coupling resistance is held contant by the control loop varying the plasma position (e). The generator match (d) is maintained by the frequency matching (f). The plasma radial position control has been described in [17].

2.4 *Control enhancements for current drive with the A1 antenna*

The required antenna directivity for the initial Fast Wave Current Drive (FWCD) experiments on JET with the A1 antenna was achieved by relative phasing of equal antenna conductor currents at other than 0 or π, nominally $\pi/2$, giving the desired asymmetric radiated spectrum, where k// is of the order 4m-1. Circulating power from one conductor to the other as a consequence of the power phase lead and the coupling between the antenna conductors results in asymmetric coupling resistances, and since the currents are equal, requires asymmetric power outputs from the amplifiers.

Fig. (17) shows the variation in calculated coupling resistance when the phase between the conductor currents is varied in a simplified antenna model. Curves (a-b) are for a nominal coupling of 5 ohms, and (c-d) for 8 ohms. In the worst case at the lower coupling when the circulating power cancels the radiated power required for one conductor,(eg where curves c or d cross the x axis), the power available to the plasma will only be half the plant capability, one amplifier output being zero. Note that the 'negative' coupling resistance shown (representing negative generator power) is not practical, as the tetrodes cannot act as a power "sink".

The JET matching control system was constrained by the original amplitude control system which imposed a symmetrical match, only possible at 0 or π phase, by imposing equal power outputs from the amplifiers, i.e. no circulating power. Refer to Fig. 12. To obtain a match and maintain equal but phased antenna currents for FWCD experiments, the amplitude regulation control signal is derived from the main transmission line forward (Vfm) and reflected (Vrm) waves, where the vector Vfm-Vrm is proportional to the antenna current, both in amplitude and phase. The individual generator halves match independently as described in the previous subsection. In the FWCD case a differential electrical length change has to be performed by the delta phase shifters, which, although not originally specified for this, have just sufficient range when the coupling is high. By regulating to equal currents, the required power imbalance is achieved automatically at the correct match, even though the coupling resistances are unequal.

JET results [18] have shown that plasma sawtooth behaviour has been modified by $\pi/2$ phasing of the antenna currents due to effects on the current profile at the inner Q = 1 surface. In Fig. (18), curve (a) shows the RF power, curves (b) and (c) show the effect of $+\pi/2$ and $-\pi/2$ degree phasing respectively (compared to dipole), on the sawteeth (electron temperature).

2.5 *Summary of section 2.*

As a result of the modular and versatile construction of the JET ICRH plant it has been possible to enhance the original control and protection systems to cope with fast vary plasma loads and to adapt them to the needs of the physics experiments.

Matching is performed automatically and for non limiter plasma includes control of the coupling resistance by controlling the plasma position. The antenna conductor currents can be independently phased for FWCD experiments. Additional drive power limiters, and output circuit arc detectors, have prevented termination of the heating pulse and generator damage, improving the availability of the ICRH plant.

3.0 The 1992/3 ICRF system upgrade for the Pumped Divertor Phase of JET

3.1 Background.

In order to couple RF power to the smaller, vertically assymetric single null (bottom X point) plasmas of the Pumped Divertor Phase of JET, the ICRH "A1" antennas are being replaced with a new "A2" design which is radially deeper and, to obtain the desired radiated spectrum, toroidally wider. In addition, to avoid interaction between the deeper side protections of these antenna and the edge of the tangential Neutral Beams, two pairs of antennas are being located in different octants. A full description of the new A2 antenna installation is given in [3].

The new location of the antennas, now grouped in four pairs, allows an improved radiated spectrum to be obtained from the four conductors formed by the "array" of two adjacent antennas, with enhanced FWCD performance. The RF coupling between adjacent conductors, which has implications for the generator plant control (described below) has been reduced by a partially slotted septum. It cannot be eliminated entirely by a full septum as this would in addition impose unwanted lobes in the radiated spectrum.

As a consequence, approximately half of the ICRH transmission line system need re-routing to the new antenna positions, and the generator cooling systems and 33 kV supplies regrouped into new pairs that correspond to the new antenna configuration. In addition a new tritium containment secondary gas barrier near to the antenna end of the transmission lines is included in the modifications.

3.2 Control System Upgrade

The new antenna configuration requires an upgrade of the amplitude, phase and matching control of each generator. The revised specification of these controls is shown in table 5. Mutual coupling between each pair of adjacent antennas forming an array means that the amplitude, phase and matching controls of adjacent generators (4 outputs) must also be linked, see (Fig. 19). As was the case with the two amplifiers feeding the two conductors of each A1 antenna, independent power restriction or tripping of one amplifier affects the match of the other, also resulting in a trip or power restriction of the latter, an unstable situation. Combining or linking the controls of each pair of amplifiers provided a satisfactory solution, and this facility will be extended to groups of four amplifiers.

Individual control of the RF currents in the antenna straps both in amplitude and arbitary relative phase for FWCD (as described in section 2 above) will also be extended to groups of four amplifiers. New control algorithms are required to maintain matching whilst allowing variable relative phase and therefore effectively a different coupling resistance on each of the four antenna straps. In addition the upgraded electronics will include the control of the circulating power transfer device called a conjugate box (see below) which optimises the generator power availibility. Improved arc protection for the antennas will also be included in this control upgrade.

One of the problems found in operation is that of discriminating between

a) damaging arcs or disharges in the antenna and vacuum feedthrough (which can only be extinguished by suppressing the RF power momentarily), and
b) high reflected or reverse power due to eigen modes, plasma variations, and cross plasma coupling from other antennas, which do not require supression of the forward power.

If the RF wave damping in the plasma is insufficient, or when the antenna-plasma distance is large, creating a "duct" around the plasma, crosstalk exists in the form of energy transmitted from one antenna to another, and appears as incoherent reflected power to the generator control and measurements. Even if the sources are sychronised, this reflected power remains incoherent because of random

amplitude and phase modulation by the plasma.

Until 1992 envelope detection was used, and the total of this reflected energy often exceeds the reflected power trip level, when all the generators are run at equal power, and the cross-talk is high. It would appear that the maximum power is independent of the number of generators curve (c) in Fig. (6). Fig. (20) shows an example of the magnitude of such crosstalk. With generators, 1D and 5D powered at different times, the reflected signal voltages of the unpowered generators 2D, 3D and 6B are shown. Note the assymetry between the amount of coupling between pairs of generators and also between the up and down parts of the same antenna 6B, due to plasma position. (The generator numbering refers to the JET octant and sector). Assymetry of the reflection coefficients of one antenna caused the generator differential trip to operate. Note also the peak in excess of 1.4 kV on 2B from 1D, a reflected signal aproaching 0.3 of the trip level from only one other source. Raising the trip level to avoid the interference risks undetected 'real' arcs in the antenna and consequential damage.

This crosstalk was also above the threshold of and interfering with the "hold" circuits of the frequency and phase feedback loops, Fig. (3), such that if a generator tripped, crosstalk from the others would ensure that its held match settings were lost and it would therefore not recover during the pulse. These problems have already been partially overcome by using more robust thresholds and timing for the hold circuits.

The new protection circuits which operate the trip will include synchronous detectors and narrow band filtering. The generator reflected power signal will first be converted to an intermediate frequency of approximately 1.3 MHz which will allow filtering to eliminate energy from generators on adjacent frequencies. Narrow band (20 kHz) pseudo-synchronous detection (requiring the presence of the carrier), will provide further filtering of close-to-carrier noise and crosstalk from the plasma. The circuitry takes advantage of ten years advance in "chip" technology, to replace outdated electronics, and also of successful experience with a similar system used in the JET Lower Hybrid Current Drive power plant. In addition the arc detection system will be tested automatically in the low power pedestal immediately before every heating pulse as a precaution against electronic failure.

3.3 Transmission Line Reconfiguration

The transmission line system design at JET has remained substantially unmodified since its initial installation with the exception of additions to the range of ceramic insulators, and new routings to suit antenna position changes. Since [6], additional ceramics have been designed to give improved voltage standoff in the test load switch and, for the 1992/3 upgrade described below a secondary vacuum containment gas barrier near the antenna end of the transmission line (see Fig. 21). The capacitor tuning stubs near the antenna (Fig. 2) have since become incompatible with the wide range of operating frequencies needed for the JET programme and the ICRH automatic matching system. However they provide a useful "emergency" facility for enabling onesided operation of a possibly defective antenna by allowing a voltage null to be tuned to any point on the defective feed-through transmission line. The stubs included an in-line coaxial switch which contacts directly the "through" transmission line at a "T" junction so that in the open position the residual stub is negligible. The switches elliminated the large manual effort required to install a full set of 16 stubs at any appropriate break in the JET operating programme.

3.4 Specific Phasing Aspects for Fast Wave Current Drive.

The required antenna directivity for FWCD is achieved by relative phasing of the four conductor currents of each A2 antenna at other than 0 or π, nominally $\pi/2$, to give the optimum asymmetric radiated spectrum. As described previously in section 2, mutual coupling between the antenna conductors with this phasing causes assymetry of power inputs to the antenna (ie additional circulating power between the conductors) which reduces the maximum available drive, down to half power in the worst case.

However the inter-conductor mutual coupling is essentially a reactive term, (a small resistive part due to the plasma can be ignored), and thus can be cancelled by a

high power loss-less compensation network containing an equal reactance of opposite sign elsewhere in the antenna feed system. This "conjugate box" network is so called because its transfer characteristics are the complex conjugate of the antenna.

In the special case of a toroidally continuous multi-element (m) antenna array, the power loading of each strap remains constant independent of Ø, the relative RF current phase between them, only when all straps are equivalent, eg $m\emptyset = n\pi$, since the circulating power is identical for each strap and not seen by the feeds. In the A2 case of 4 conductors, circulating power must be supplied in addition at one end of the array and be absorbed at the other. Because of the symmetry of the system the power can be re-circulated via a lossless network connecting between the transmission lines. The ideal case, one box between each pair of lines is impractical in the JET case (Fig. 22a) but a compromise which works over most of the frequency and phase range is a single compensator between lines 1 and 4 (Fig. 22b). The predicted performance of the system is shown in Fig. 23, showing (i) no compensator, (ii) a 2 line compensator, (iii) a 4 line compensator.

The design of this "conjugate box", required a simulation of the A2 antenna and its behaviour for FWCD in combination with such a network. Work by JET and ORNL using plasma, antenna and network modelling codes for predictions of the launched RF power directivity and wave absorption by the plasma is described in [19]. This includes FWCD efficiency and profile calculations. These combined codes also predict the generator loading and thus the matching control dependence on the phased antenna strap currents.

3.5 *Conjugate Box Power Compensation System Practical Design*

A practical design of conjugate box is fabricated from a quarter-wave 3 dB (symmetrical) power combiner with two ports terminated by variable reactive elements, in this case capacitors, Fig. 24. The compensation is frequency dependent and a compromise in the operating range is achieved by design adjustment of the various connecting lengths shown. For the JET plant, four conjugate box systems are required, connecting lines 1 and 4 of each of the four-conductor antenna arrays.

The inline switches and the capacitors and two of the required four suitable 3 dB power combiners are already available at JET, Fig. 25. These combiners were originally purchased in 1986 to combine the four outputs of two generators on to one A0 antenna for high power tests [5]. The capacitor tuning stubs were originally purchased for increasing the efficiency of the A0 antenna in the low coupling quadrapole mode [4]. The inline switches allow the conjugate system to be disconnected during normal (high coupling) plasma heating.

3.6 *Summary of section 3*

The ICRH system for the pumped divertor phase of JET includes new "A2" antennae with a revised layout inside JET. The associated generator control system upgrade will include new algorithms for matching and independent antenna conductor current control for Fast Wave Current Drive experiments. Additional circulating power compensation is also added to the antenna transmission line system. The arc detection and protection currently will be more able to discriminate between arcs and plasma cross coupled interference from other generators. It will also include an automatic low power check prior to every JET pulse.

Conclusions

Because of its flexibility and versatility, the original modular concept of the JET system architecture has been successful in allowing the continual development of the generator plant to cope with the more stringent load conditions imposed by the evolution of the ICRH physics programme on JET.

Over 22MW of ICRF heating at the plasma centre has been achieved with the generator plant running at 26.3MW, 82% of its design test load capacity. The modularity means that emergency incidents such as a tetrode replacement only reduce the power capacity of the plant to 87% and do not usually affect the physics programme.

The control of the ICRH generators is highly automated and the plant is operated entirely remotely from the JET control room with a minimum of staff. Matching the generators to the plasma load is performed automatically on line during the JET pulse. For non-limiter plasmas a constant coupling resistance can be maintained by feedback control of the plasma horizontal position, which has allowed RF heating during "L" to "H" mode transitions. If required by the experimental programme, the operating frequency or other parameters can be changed easily between plasma shots by down loading stored plant settings.

Independent amplifier operation allows antenna conductor currents to be phased at other than 0 or π (whilst still maintaining a match) permitting Fast Wave Current Drive Experiments using assymetric k// spectra. New matching algorithms and a circulating power compensation system for the four element A2 antennas are part of the plant upgrade for the Pumped divertor phase of JET.

In comparison with the JET ICRH system, the requirements for the ICRH system of an experimental reactor scale device will be higher power, quasi-continuous operation and higher DC-RF conversion efficiency. All the high power RF components to do this already exist or require little development, but innovation is required to achieve plant operation with near 100% availability of the heating power, still keeping experimental flexibility, and operating at a higher conversion efficiency, >85%.

A future plant design must use a more sophisticated model analysis of transients and peak voltages arising from the fast varying plasma load including arcs or discharges within the antenna itself, in order to design the plant protection and to make its the plant performance independent of antenna-load behaviour.

Near 100% availability of heating power will require faster tuning devices, matching the response time of the plasma, and new control algorithms to match multi-element arrays.

Further development of the antenna protection system is needed. Transient variations in the plasma load, caused by eigen modes or cross-coupling from other antennas, are difficult to distinguish from the variations caused by discharges in the antenna itself. To stop the heating pulse only when there is a real risk of antenna damage is a demanding task for the antenna protection.

The success of the JET ICRH plant design and its continuing development makes an esential contribution to the critical design issues of a reactor relevant ICRF system.

References

[1] J Jacquinot et al., JET Recent Results on Wave Heating and Current Drive. Consequences for Future Devices. Europhysics Topical Conference on Radio Frequency Heating and Current Drive of Fusion Devices, Brussels, July 1992, to be published.

[2] J Jacquinot et al., JET Results With Both Fast and Lower Hybrid Waves, Consquences For Future Devices. Physics of fluids, special issue, to be published.

[3] A Kaye et al., Present and Future JET ICRH Antennae, this edition.

[4] T J Wade et al., The JET ICRF Power Plant, Proc 13th Symposium on Fusion Technology, Varese, Italy 1984, pp 727-732.

[5] R J Anderson et al., Overview of the JET ICRF Power Plant operation and development.. Proc 14th Symposium on Fusion Technology, Avignon, France 1986 pp93-99.

[6] T J Wade et al., The Technology of the Upgraded JET ICRF Heating System, Proc 7th topical meeting on Technology of fusion energy, Reno, Nevada 1986, pp 1398-1403.

[7] T J Wade et al., Automatic ICRH Power Coupling to any Plasma In JET, IEEE/NPS 12th Symposium of Fusion Engineering, Monterey, 1987, pp 1200-1203.

[8] T J Wade et al., High power (22 MW) ICRH at JET and developments for next step devices , IEEE/NPS 14th Symposium on Fusion Engineering San Diego 1991, pp 902-907.

[9] A Kaye et al., The JET Project: Radio Frequency Heating System. . Fusion Technology vol 11 No. 1 Jan 1987, pp 203-234.

[10] Lawson et al., Megawatt Power for Ion Cyclotron Heating, 7th Symposium on Engineering Problems of Fusion Research Knoxville Ten. 1977, pp 1125-1128.

[11] Sivo et al, Multi-megawatt Radio Frequency Power Source for Plasma Heating CEC 2nd Joint Grenoble-Varenna International Symposium on Heating in Toroidal Plasmas Villa Olmo Como, 1980, pp 621-627.

[12] G Clerc et al., ICRH Tetrodes - the new results 12th Symposium on Fusion Engineering Monterey 1987 pp1176-1179.

[13] G Clerc et al., ICRH Thomson Tetrodes : from Long Pulses to CW 14th IEEE/NPS Symposium on Fusion Engineering San Diego 1991, pp488-491.

[14] R Claesen et al., The JET Project: Neutral Beam Injection and Radio Frequency Power Supplies. Fusion Technology Vol 11 No. 1 Jan 1987, pp 141-162.

[15] P P Lallia and P H Rebut, preliminary Studies on the JET RF heating Sytem. CEC 3rd Joint Grenoble-Varenna Internation Symposium on Heating in Toroidal Plasmas. Grenoble 1982, pp 799-811.

[16] G Bosia et al., Automatic VSWR Control in JET ICRH Transmitters, proc 16th SOFT London, 1990, pp 1099-1103.

[17] E Bertolini et al., The JET project: Magnet Power Suplies and Position Control. Fusion Technology Vol 11 No. 1 Jan 1987, pp 107-109.

[18] D F H Start et al., Observation of Fast Wave Ion Current Drive Effects on Saw teeth in JET. 19th EPS conference on Controlled Fusion and Plasma Physics Innsbruck 1992, Vol II, pp 897-900.

[19] R Goulding et al., Phased operation of the JET A2 antenna arrays. 17th Symposium on Fusion Technology. Rome 1992. To be published.

Table 1

Nominal Characteristics of the ICRF Plant

Frequency Range		• 23 to 57 MHz (determined by the full field ion cyclotron resonances of deuterium and hydrogen), excluding 39-41 MHz.
8 Generators		• 4 MW output per generator module (20 s)
8 Antenna		• Beryllium bars (15° inclination) screen
		• Two adjacent loops operated with either Monopole phasing (0, 0) or dipole phasing (0, π), or a phased array (0-π).
16 Transmission lines (Generator to antenna)		• Each line 84 m long rated at 50 kV peak (dia. 230 mm, 30 Ω)
Feedback loops for		• Plasma position for constant coupling resistance.
		• RF power level or antennae RF current
		• Phase between antenna conductors. • Frequency (Δf~1 MHz) for matching • Motorised tuning stub for matching
		• Tetrode screen dissipation and anode efficiency (acting on anode voltage).
8 HVDC Power Supplies	: Output (2 tubes)	• 345 amp : 16-26kV controlled by tetrode screen and current (see also table 3).
	: Driver (2 tubes)	• 60 amp : 9-13kV (remotely preset).

Table 2

ICRH system network model (see Fig.s. 7, 8 and 9)

Coupling resistance Rc: variable	:	2-5 ohm Fig.. 9
	:	4 ohms Fig.. 7
Main transmission line ℓm	:	84 m
Generator output line ℓo	:	6.5 m
Arc position $\psi(p)$ $\pm\lambda/8$ variable at	:	V max or 2.4 m from end (conic)
Anode limit Va	:	60 kV
Capacitor limit Vc	:	26 kV
Inductor limit Vl	:	20 kV
Anode current Ia (pk RF)	:	272 A
Unit line loss rl	:	5.10^{-3}/m (ohms)

Generator output circuit (Fig. 8)

C1 = 130pF (anode-g2 capacitance)

C2 = 5000pF (DC blocking capacitance)

Freq	(MHz)	25	29	33	37	43	47	51	55
C3	(pF)	166	144	126	112	094	084	076	070
L1	(nH)	700	440	305	224	152	122	100	083
L2	(nH)	490	437	400	370	338	322	309	295
L3	(nH)	210	189	176	166	156	151	147	142

TABLE 3

ICRH Control and Protection System

Category		Value	Response Time
(1)	TERMINATE THE PULSE.		
-	Tetrode arc crowbar protection	Overcurrent	10 μs
-	maximum trip count exceeded.*	(ρ = 0.5)	255 times
-	Tube dissipation high, limiter not working.	1.5 MW	5 ms
(2)	POWER TRIP (hold settings and recover)		recovery 1%/ms
-	Arc in end stage circuitry*	UV light	2 ms off/20ms on
-	too high reflection coefficient	ρ = 0.5	2 μs off/20ms on
-	too high difference in reflection coefficients between the two antenna feeds.*	(ρ1~ρ2) = 0.5	2 μs off/20ms on
-	*phase of reflection abnormal.*	Δø ≥ ±90°*	*not installed*
(3)	LIMIT THE OUTPUT POWER [PSU trips shown in brackets]		
-	Anode dissipation	1.3 MW	1→5 ms
-	Screen grid current	4 A [20 A]	0.5 ms [>20 ms]
-	Control grid current*	5.5 A [6 A]	0.5 ms [10-20 ms]
-	Anode current [both tubes]	160 A [345A]	1-5 ms
-	Maximum RF voltage on antenna and transmission line (set on operation)	30-40 kV	0.5 ms
-	RF forward voltage**	≃ 2 MW	1-5 ms
-	RF reflected voltage**	130 kW	1-5 ms
-	Drive Power* replaced by control grid above.	(100 kW)	(0.5 ms)
(4)	REQUESTED VALUES (operating as control loops)		
-	Power, *or antenna currents* *.	± 0.25 dB	
-	Relative Phase	±5°	
-	Nominal Frequency	10 KHz ± 1 KHz	
-	Coupling resistance via plasma position control*	0.1 Ω steps	
(5)	AUTOMATIC.		
-	Matching. Uses stubs plus frequency or trombones.	see separate	description
-	Anode voltage to minimise anode dissipation (linked to screen current limiter above)	Ig2 = 2.5A	200 ms 18-26 kV

Table 4

Derivation of Model Calculations

JET matched operating frequencies are given by:-

$$f = \frac{n\, c \tan^{-1} \sqrt{(Rc/30)}}{2\, \pi\, \ell m}$$

where $c = 3 \times 10^8$ m/s;

harmonic of line resonance n is given by $13<n<32$; ℓm, Rc are from table 2.

The normalised admittance of an arc on the matched side of the stub is derived thus:-

Normalised admittance of plasma load just before stub (stub will cancel reactance)

$$y = \frac{1+j(yc-1)}{\sqrt{yc}}$$

where yc = 30/Rc (given in table 3);

angle of load admittance $\psi(a) = \psi(y) + \psi(p)$;

where $\psi(p)$ represents position of arc (eg at conic).

Arc reflection coefficient

$$\rho a = \frac{30-(rl.\ell m)}{30+(rl.\ell m)} \qquad \ell m \text{ from table 2}$$

admittance of arc at stub

$$ya = \frac{1-\rho(a)\, e^{j\,\psi(a)}}{1+\rho(a)\, e^{j\,\psi(a)}}$$

admittance of stub

$$ys = \frac{-j\,(yc-1)}{\sqrt{yc}}$$

Thus admittance of arc at generator side of stub

$$yg = ya + ys.$$

TABLE 5

Upgraded ICRH Plant Control Performance Specification

Frequency	
Operating frequency range (fo) in 8 bands of 4 MHz	23-57 MHz
(39-41 MHz are not used)	
Inband frequency deviation (Δf)	200 kHz
Frequency regulation better than	1 KHz
(Accuracy and Stability for both fo and Δf)	
Frequency loop time response to a square pulse (Δf = 500 KHz)	1 ms
Overshoot	15%
Protection	
Limiter intervention time	<1 ms
U/V arc detection time typically	2 ms
Trip intervention time	20 μs
Trip re-application time	20 ms
Ramp up time to full power on re-application (clock synchhronised)	80 ms
Reflection coefficient detector disabled below amplifier output power of	20 kW
Generator Performances Parameters	
Amplitude Regulation	
Dynamic range	2.5 MW-5 kW
Minimum power for regulation	5 kW
Regulation accuracy (at any power level)	± 5%
Closed loop response to square pulse (to 5% of reference)	400 μs
Amplitude overshoot	< 5%
Maximum Modulation Frequency (square wave excitation)	100 Hz
Phase Regulation	
Phase loop dynamic range (any phase offset)	360°
Phase regulation accuracy and stability	± 5°
Phase linearity	± 5°
Phase loop time response to a 180° step (to ± 5°)	100-μs
Overshoot	< 15%
Phase modulation	
Dynamic range (any phase offset):-	360°
Modulation of Operation	
i) Maximum output power	± 15° variation in set phase allowed for plasma matching.
	± 15° variation in power between amplifiers
ii) Phase control	Normal 5% tolerance on set amplitude and phase.

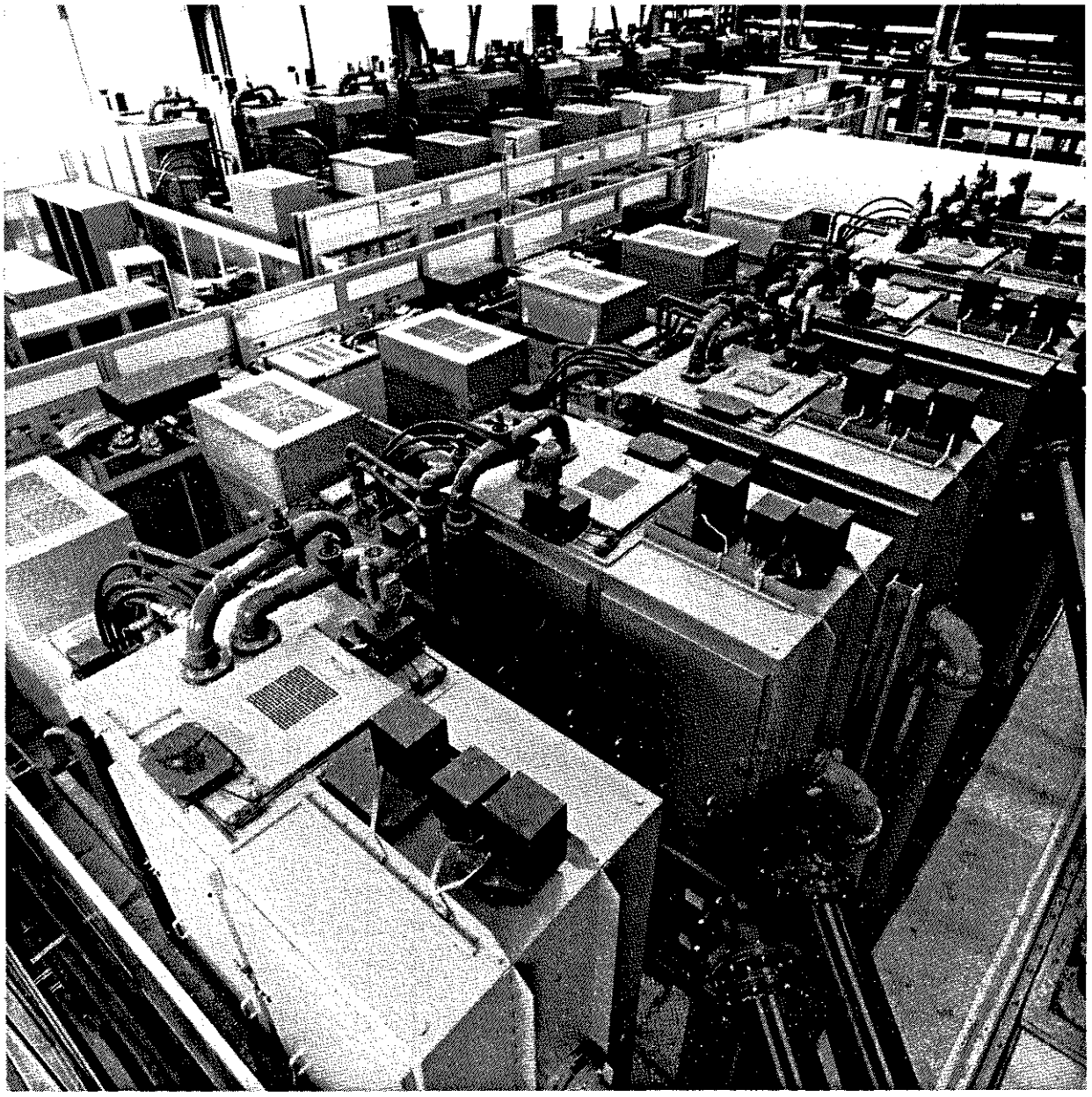

Fig.. (1) Eight installed ICRH gererator units at JET.

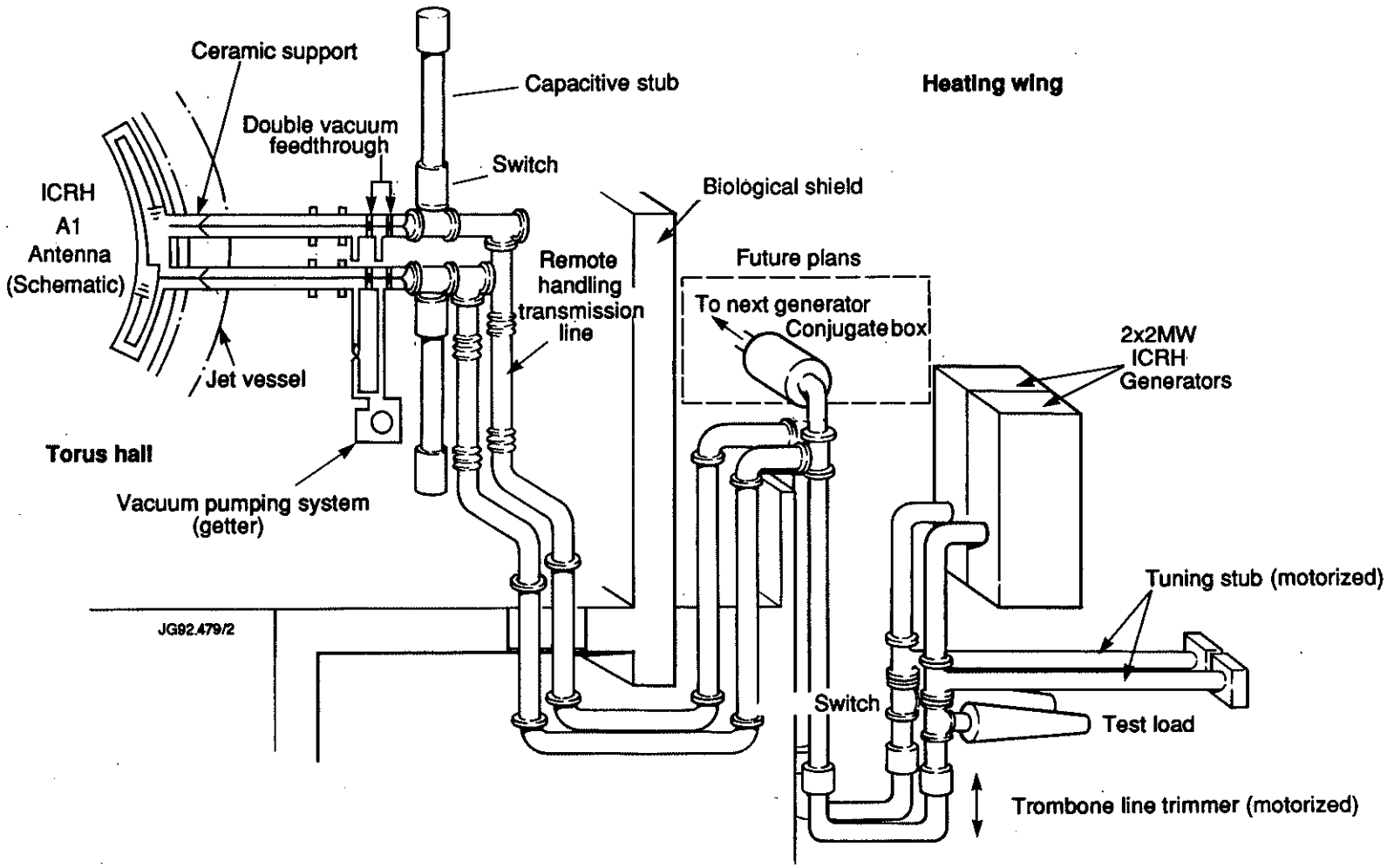

Fig. (2) Schematic of one JET ICRH generator-antenna unit.

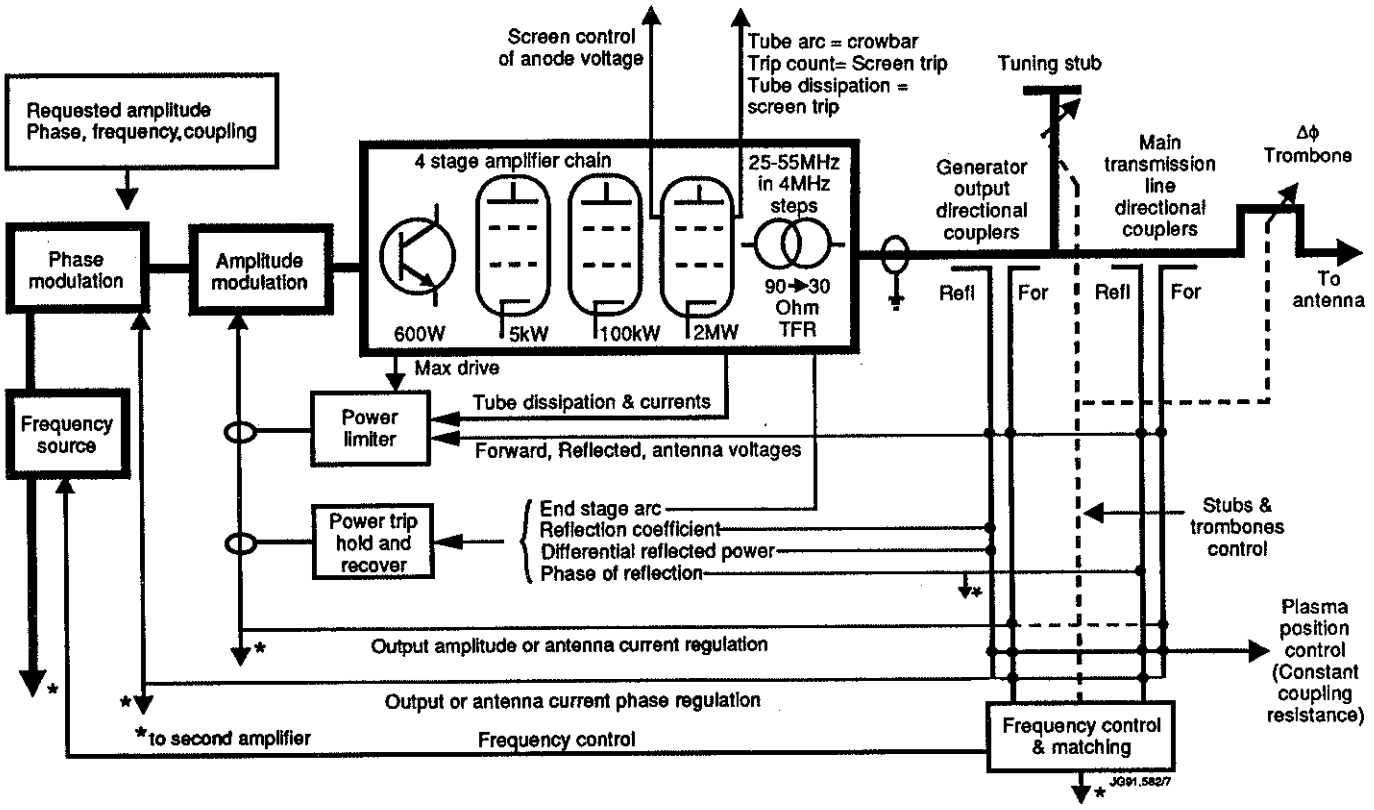

Fig. (3) Schematic of one ICRH Amplifier chain.

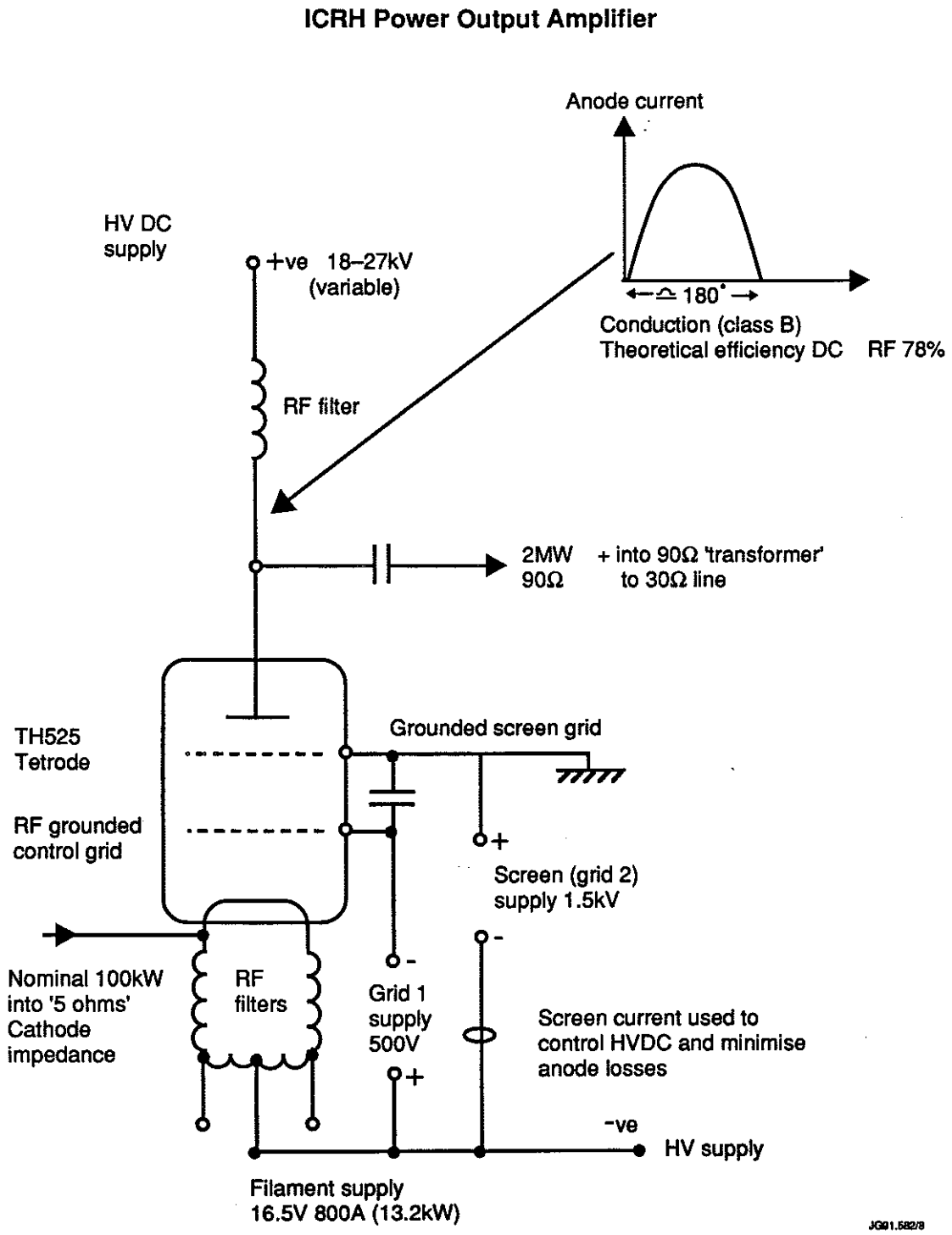

Fig. (4) Circuit diagram of JET ICRH tetrode power output stage.

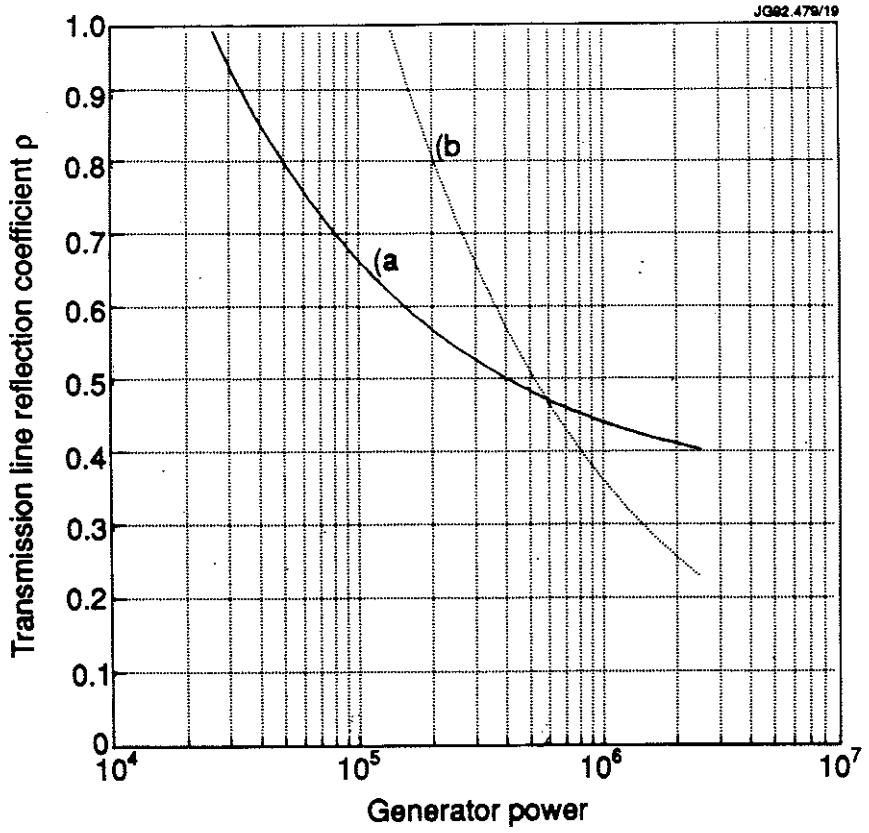

Fig. (5) Generator reflected power trip (a) and limiter (b) thresholds.

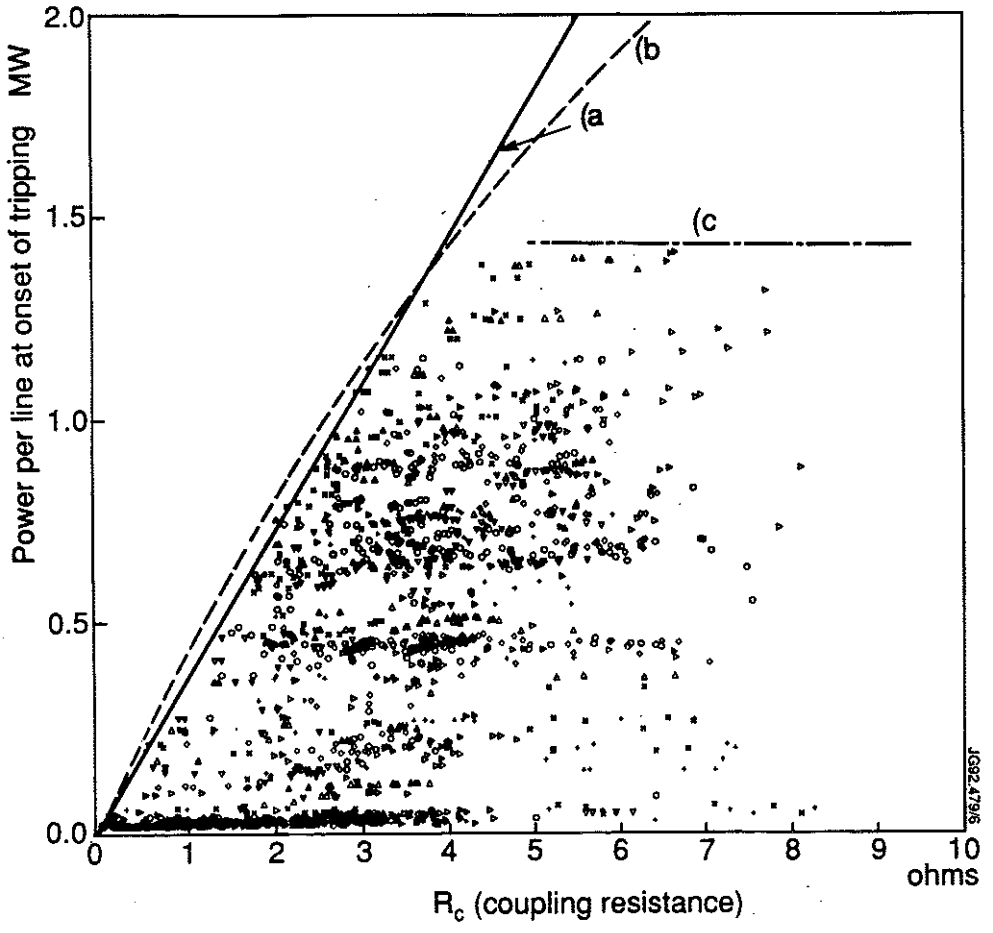

Fig. (6) Generator powers v coupling at onset of tripping at 42 MHz (1988 data).

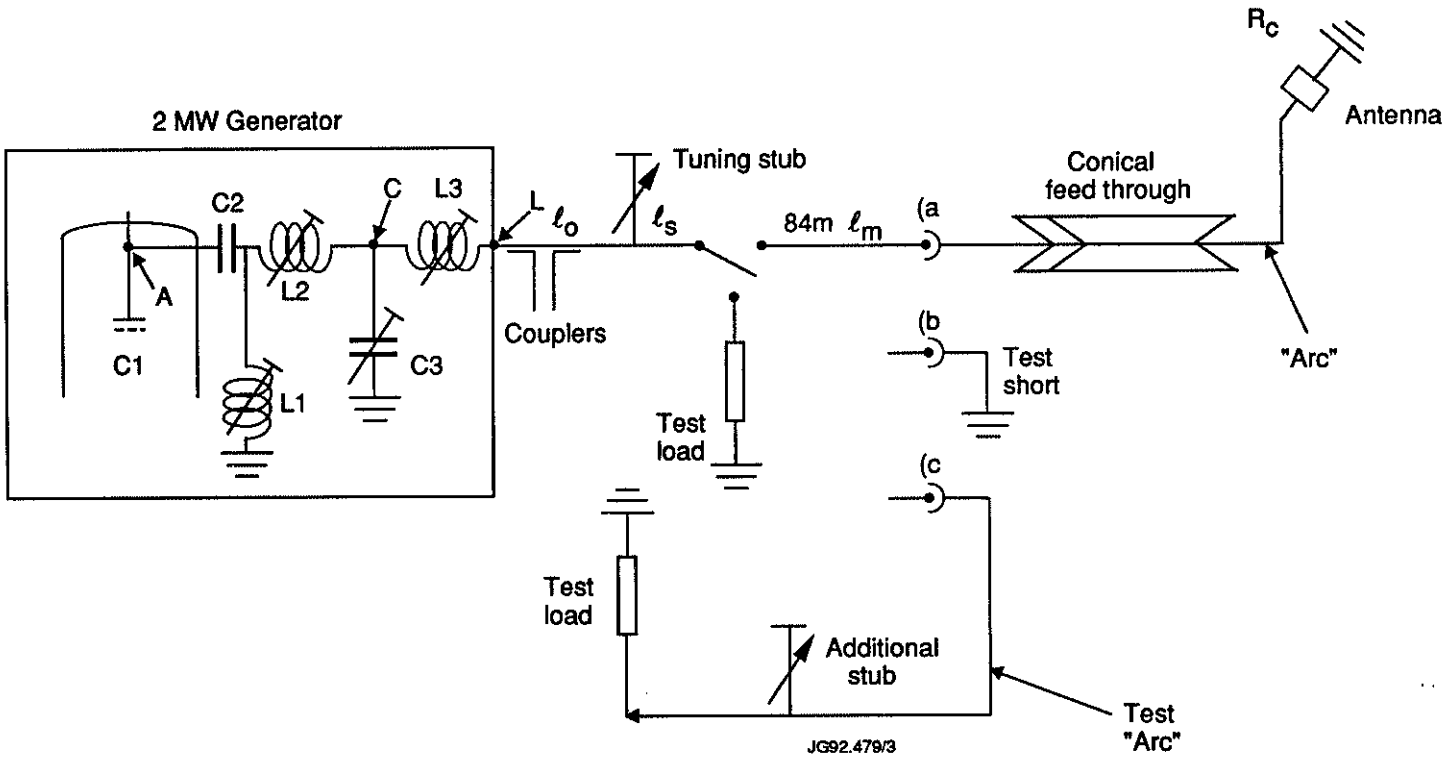

Fig. (7) Circuit Model of ICRH system for arc simulation tests.

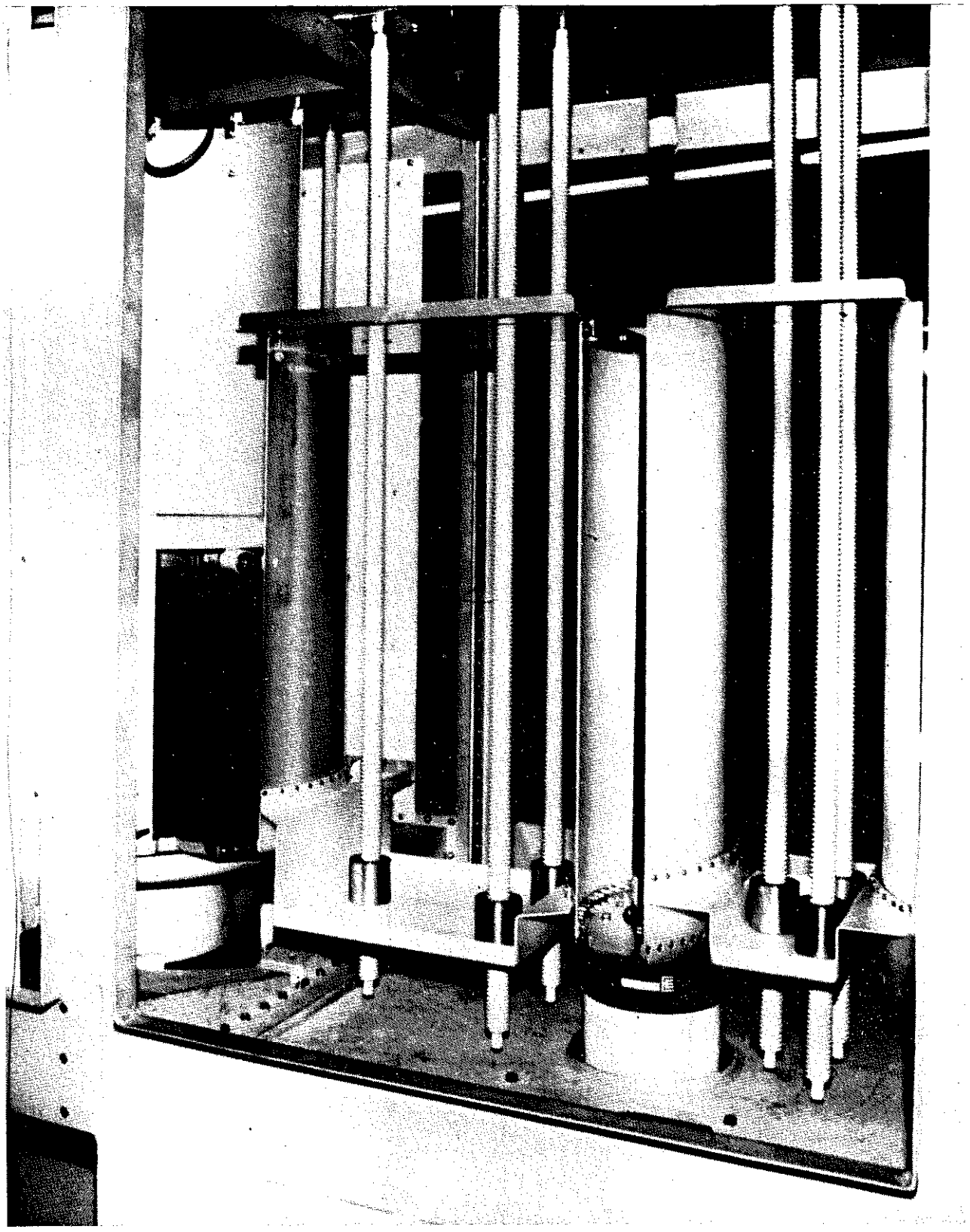

Fig. (8) JET ICRH amplifier outut transformer components.

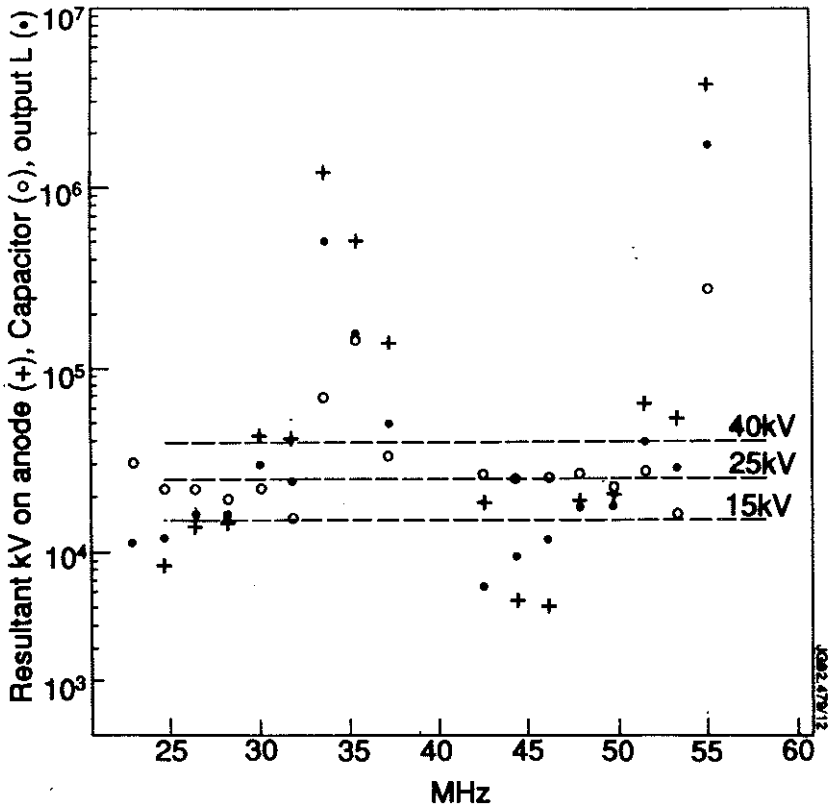

Fig. (9) Prediction of output circuit component voltages v frequency with full tetrode current after antenna arc.

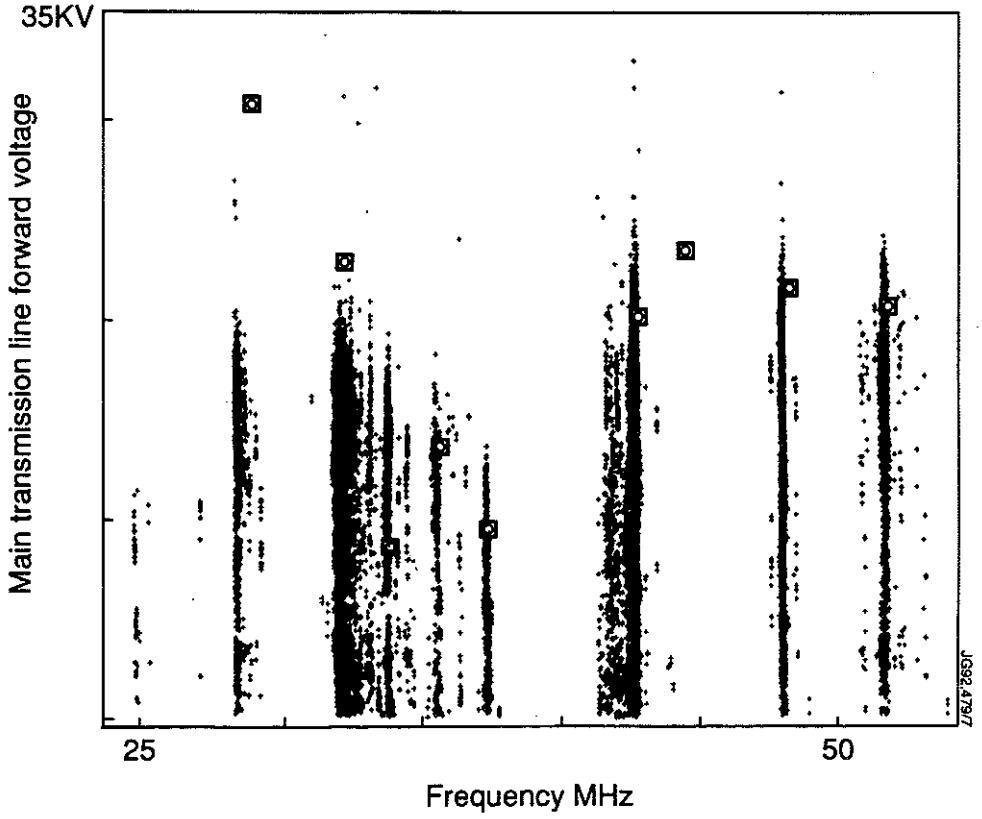

Fig. (10) Antenna transmission line voltage v frequency at onset tripping. Model and 1990 data.

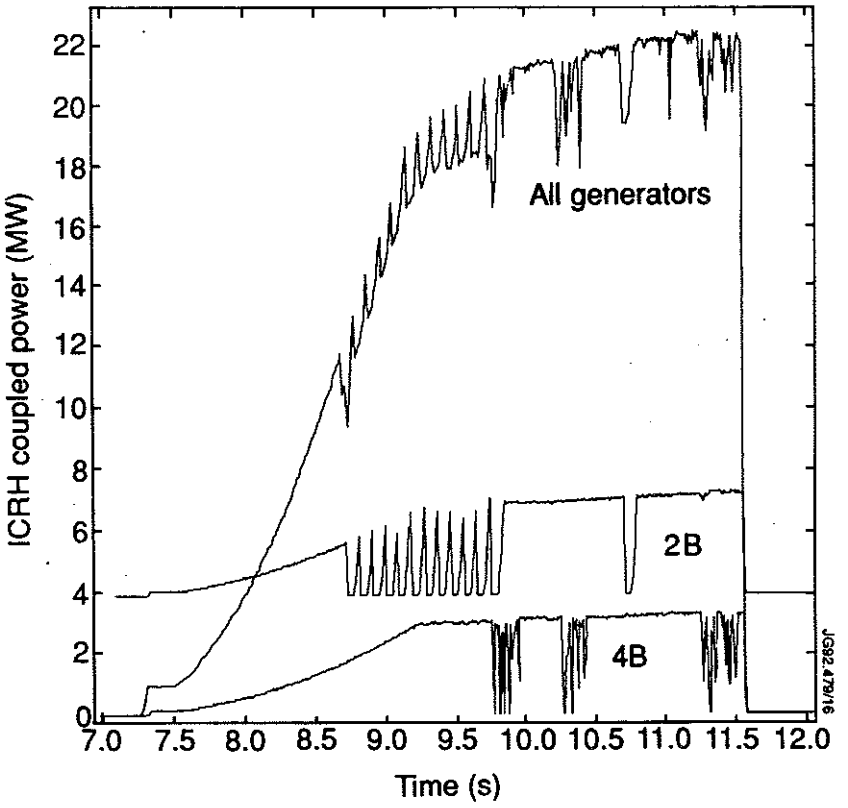

Fig. (11) JET high power ICRH pulse showing trip protection.

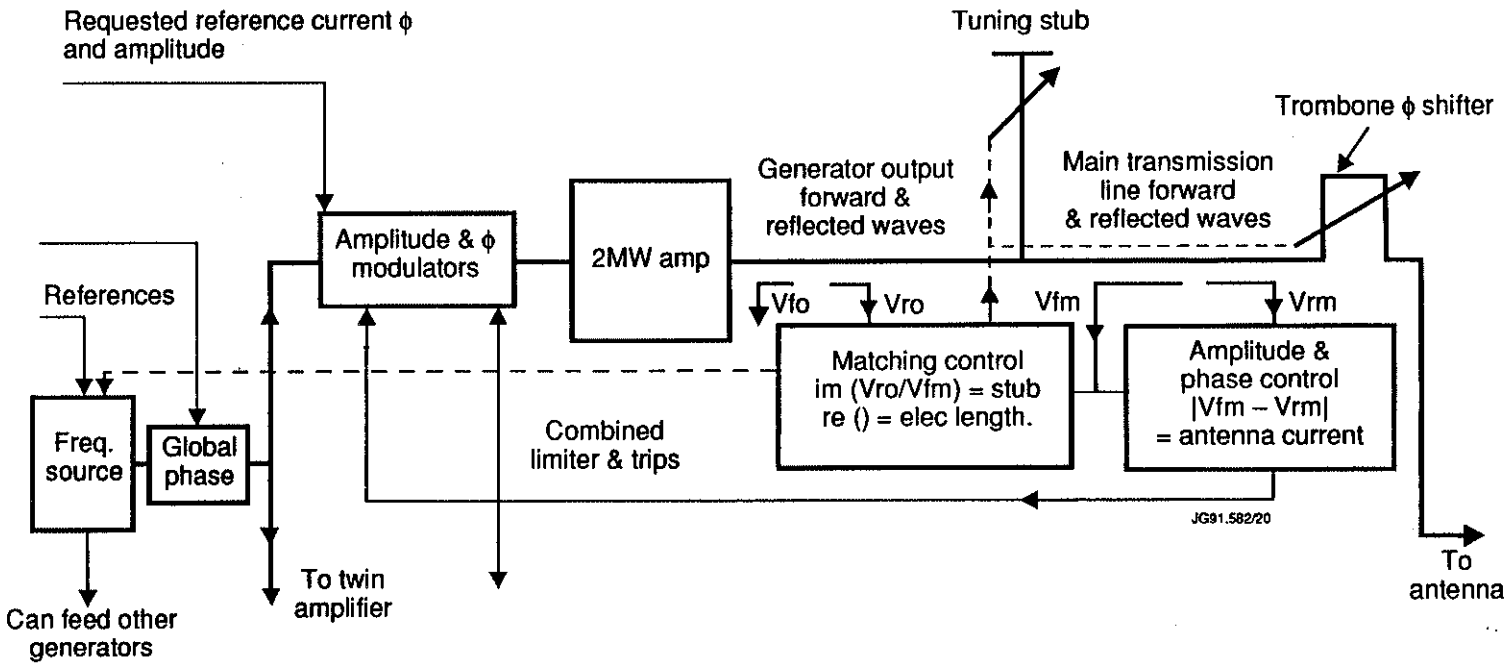

Fig. (12) JET ICRH automatic matching and antenna current control block diagram.

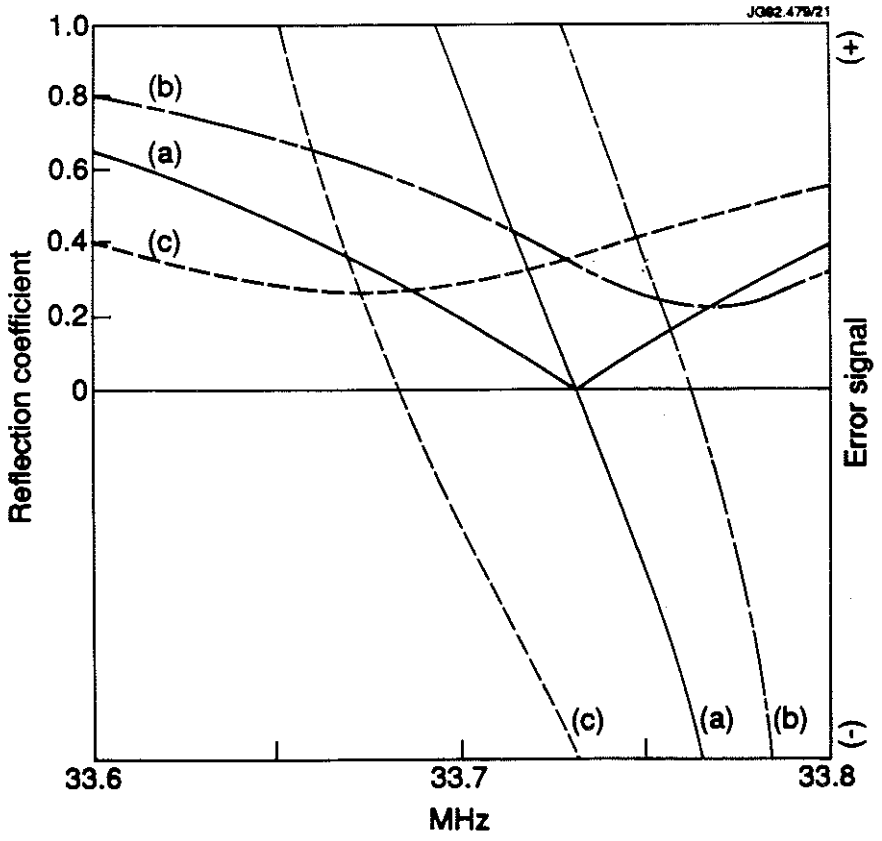

Fig. (13) Generator reflection coefficient and frequency control signal v frequency.

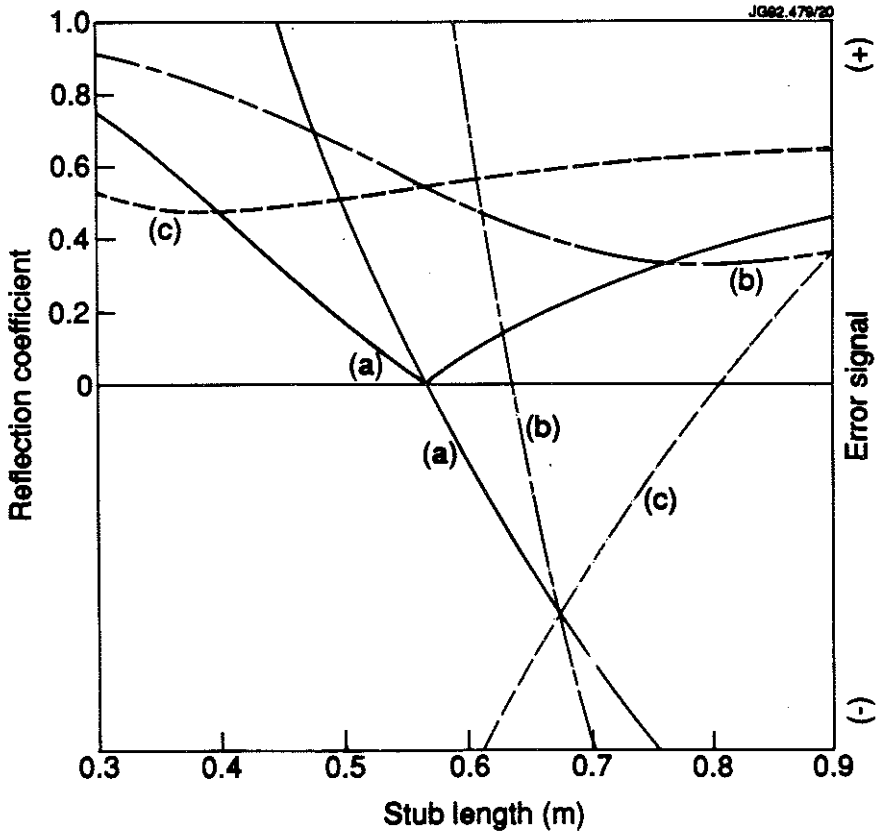

Fig. (14) Generator reflection coefficient and stub control signal v stub length.

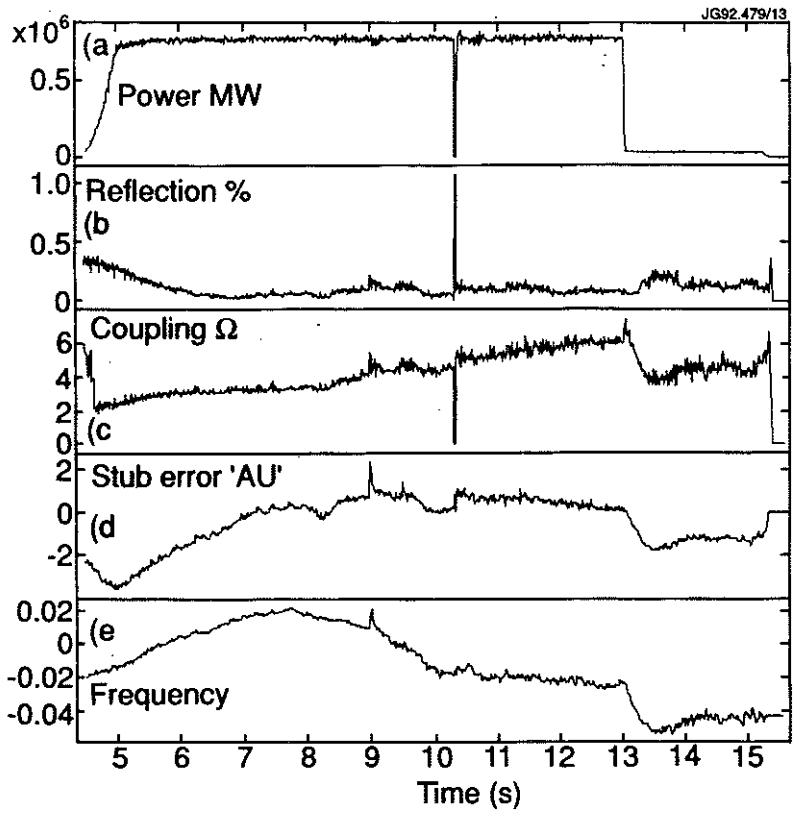

Fig. (15) JET ICRH one shot matching.

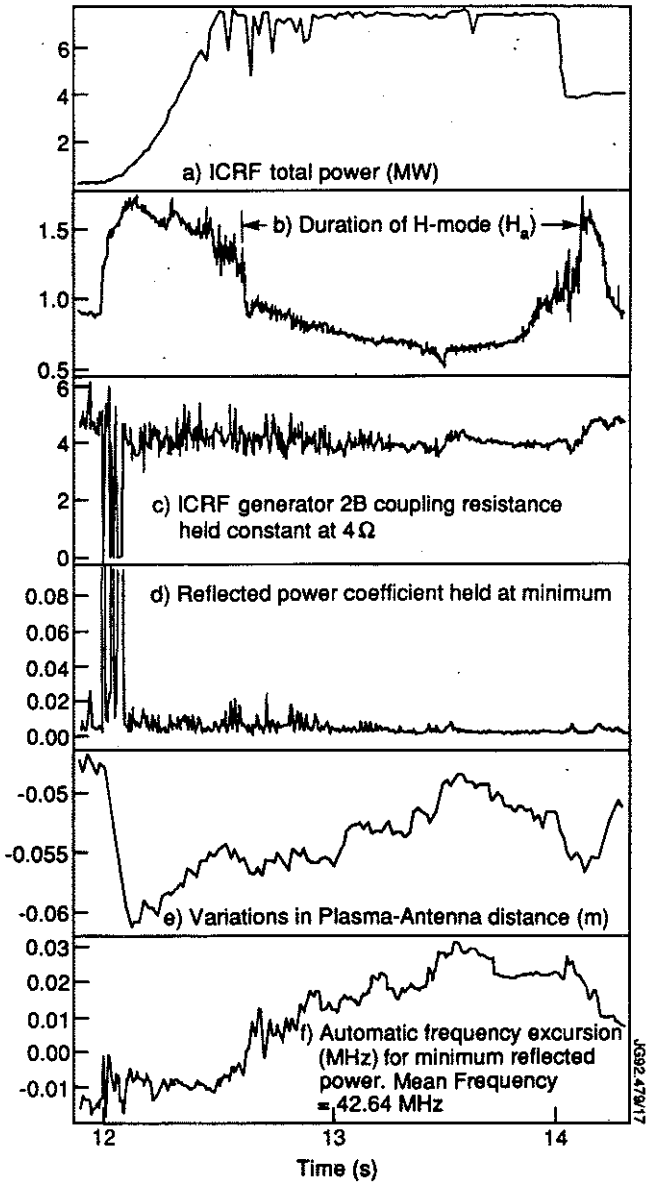

Fig. (16) JET ICRH heating of L-H mode transition.

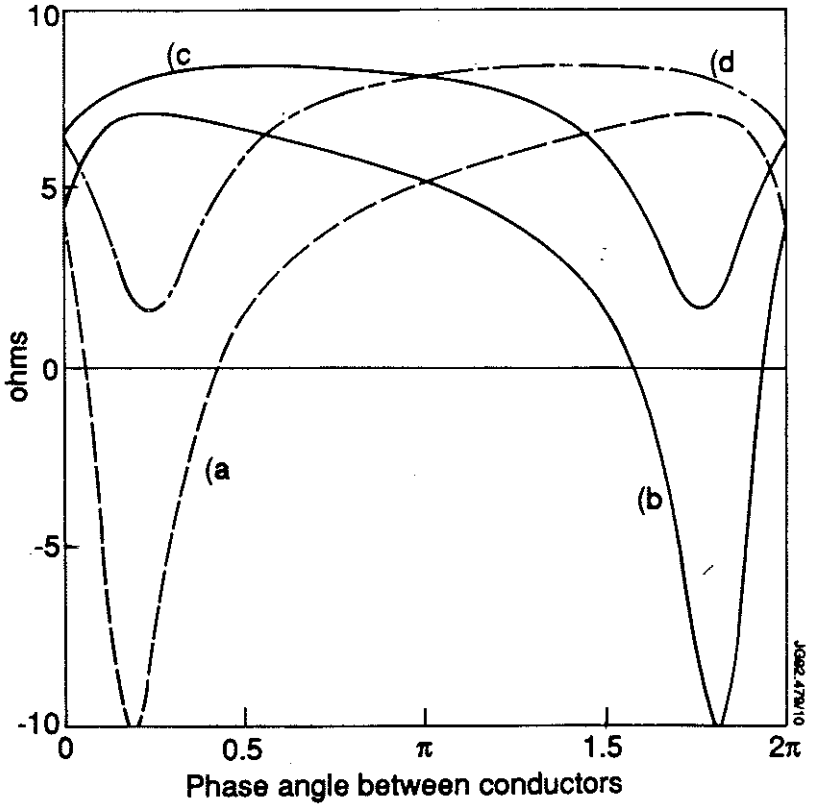

Fig. (17) Modelled variation in antenna coupling resistance v conductor current relative phase.

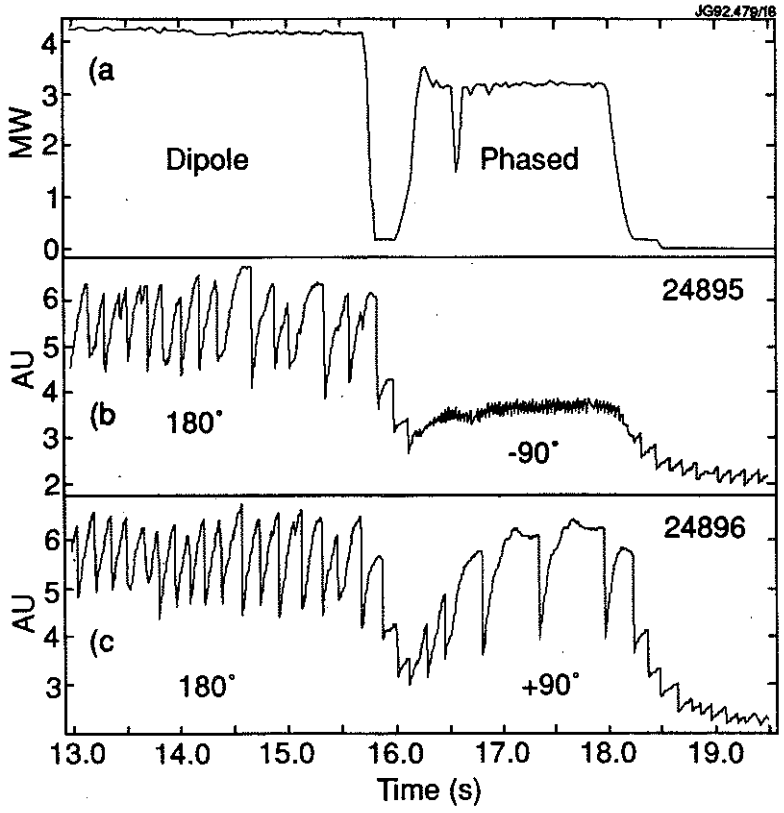

Fig. (18) Antenna current phasing effect on JET plasma sawteeth.

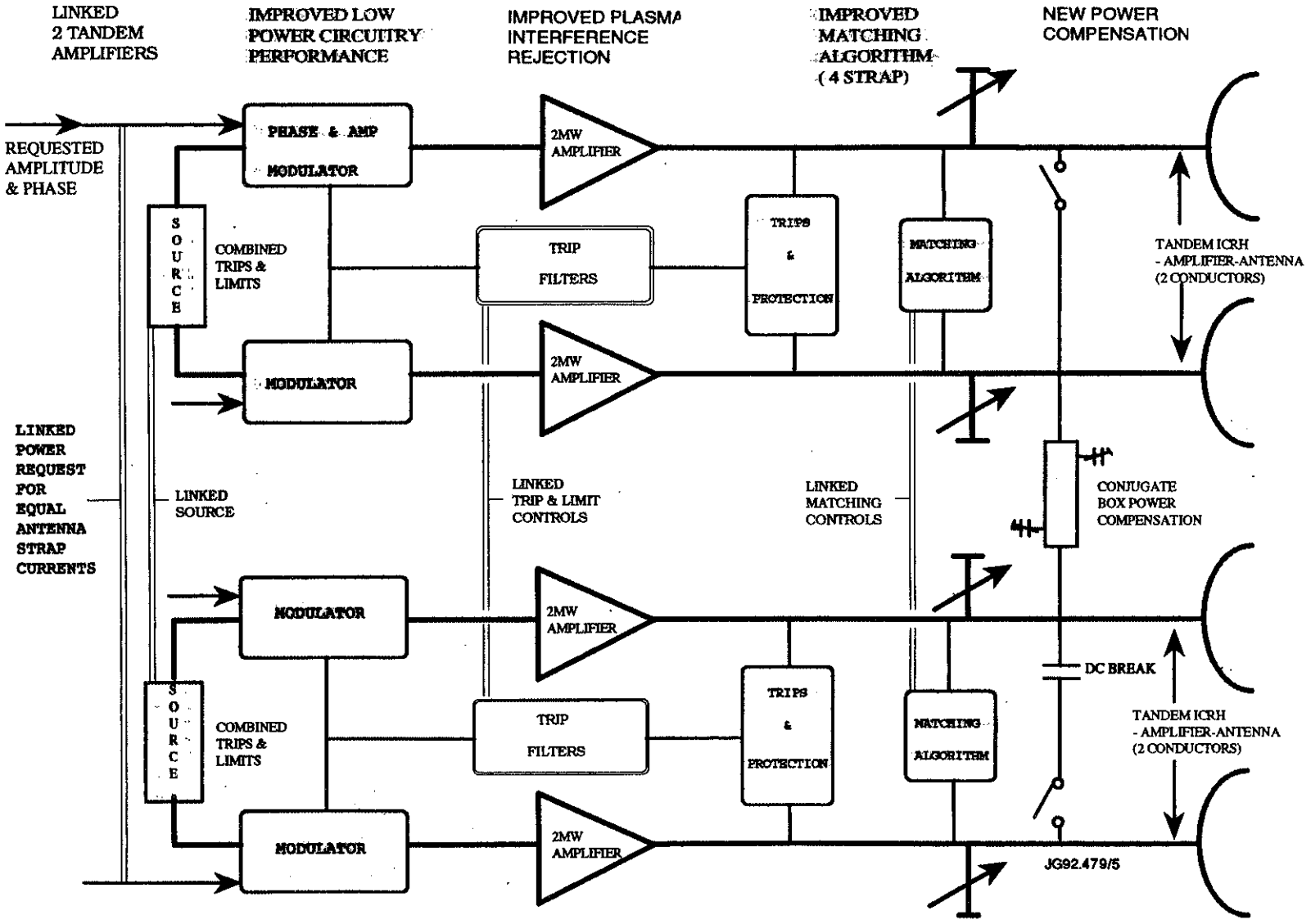

Fig. (19) Control Block Diagram of four linked ICRH amplifiers in pumped divertor phase of JET programme.

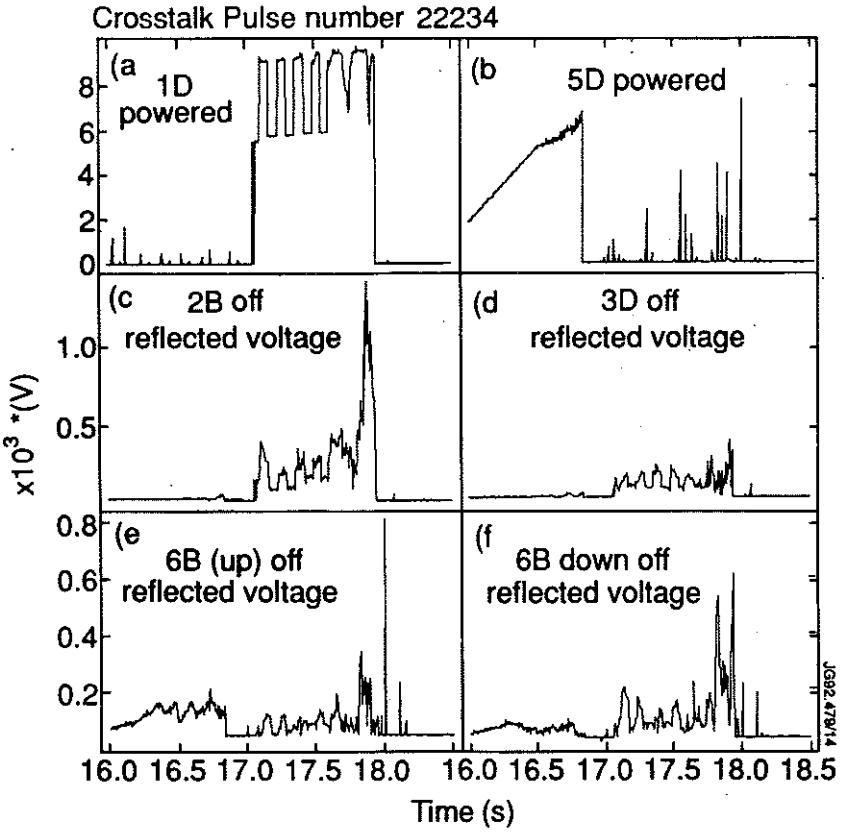

Fig. (20) Antenna crosstalk.

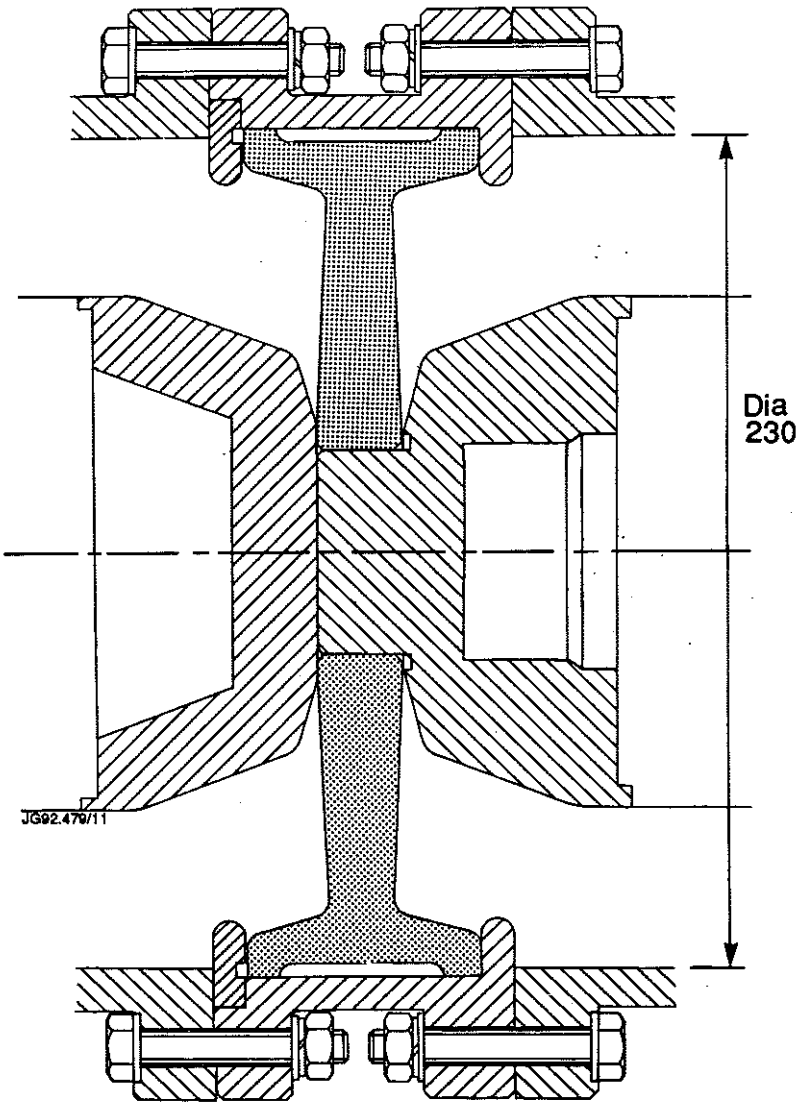

Fig. (21) New transmission line ceramic "T" support for central conductor including gas barrier.

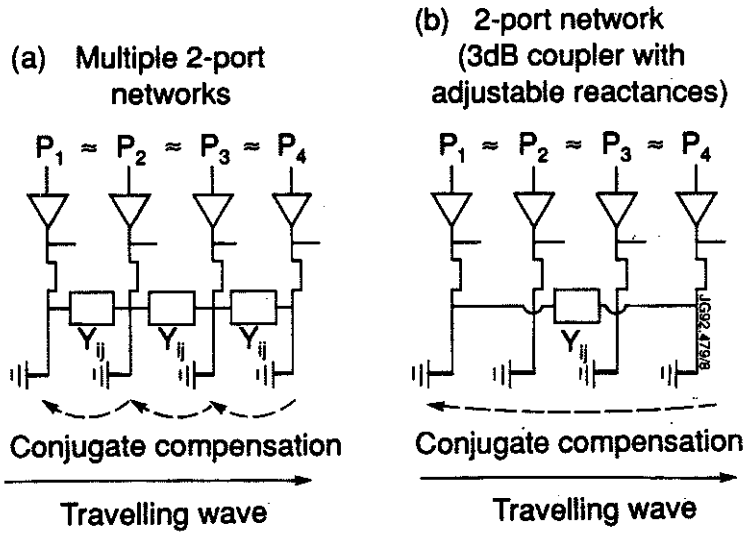

Fig. (22) Power compensation network connections between antenna transmission lines.

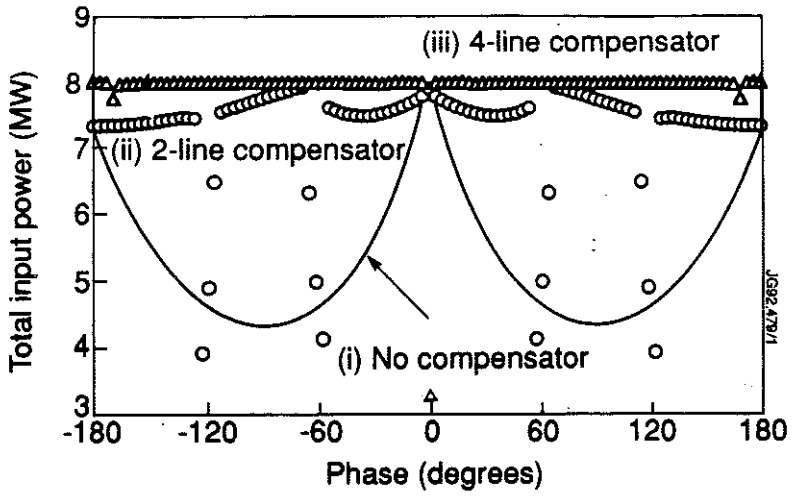

Fig. (23) Modelled maximum power capability v phase with and without compensation between transmission lines. Coupling is ~2.5 Ω and conductor currents are equal.

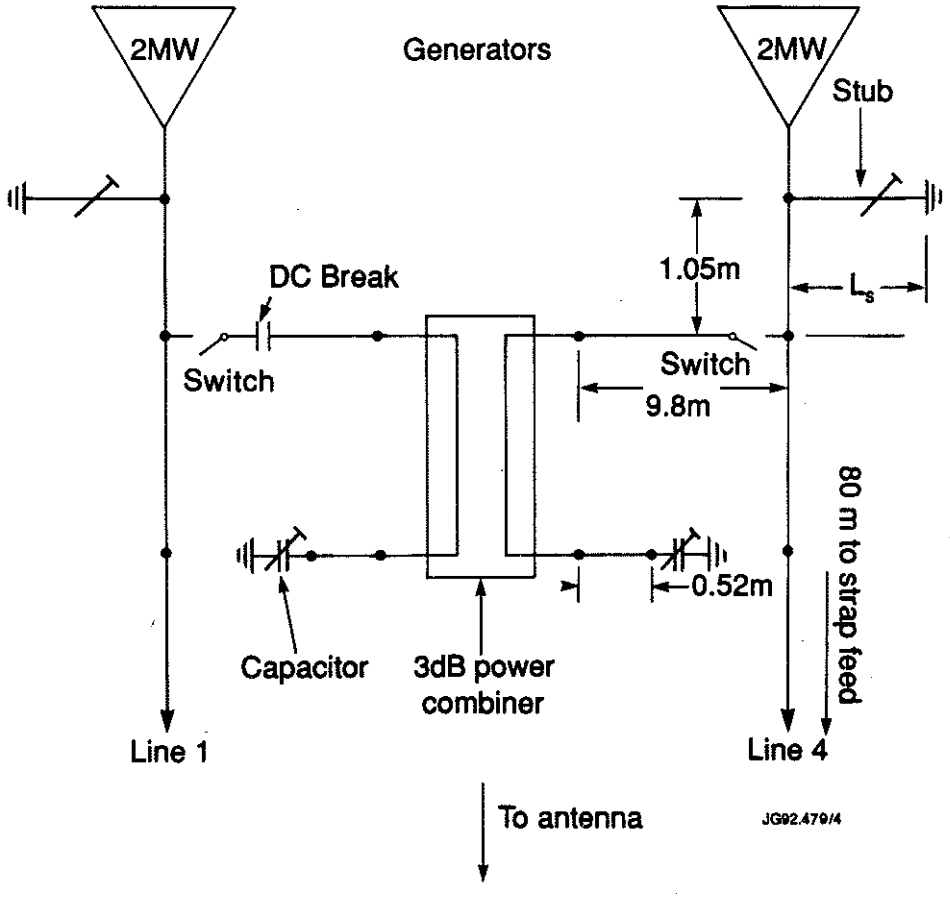

Fig. (24) Proposed practical compensation network connection on JET antenna transmission line system.

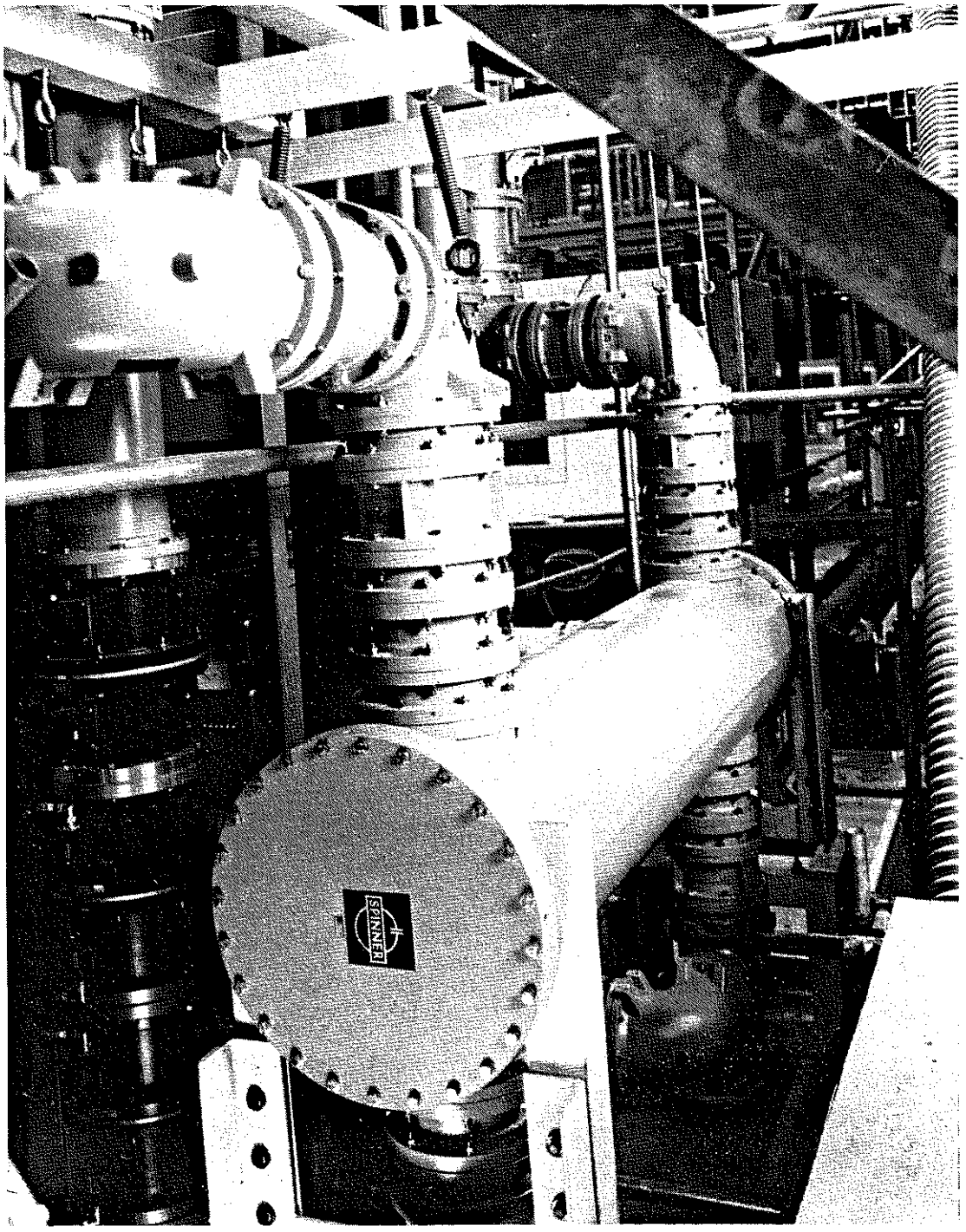

Fig. (25) A JET 3dB 4MW power combiner.

Appendix I

THE JET TEAM

JET Joint Undertaking, Abingdon, Oxon, OX14 3EA, U.K.

J.M. Adams[1], B. Alper, H. Altmann, A. Andersen[14], P. Andrew, S.Ali-Arshad, W. Bailey, B. Balet, P. Barabaschi, Y. Baranov, P. Barker, R. Barnsley[2], M. Baronian, D.V. Bartlett, A.C. Bell, G. Benali, P. Bertoldi, E. Bertolini, V. Bhatnagar, A.J. Bickley, D. Bond, T. Bonicelli, S.J. Booth, G. Bosia, M. Botman, D. Boucher, P. Boucquey, M. Brandon, P. Breger, H. Brelen, W.J. Brewerton, H. Brinkschulte, T. Brown, M. Brusati, T. Budd, M. Bures, P. Burton, T. Businaro, P. Butcher, H. Buttgereit, C. Caldwell-Nichols, D.J. Campbell, D. Campling, P. Card, G. Celentano, C.D. Challis, A.V.Chankin[23], A. Cherubini, D. Chiron, J. Christiansen, P. Chuilon, R. Claesen, S. Clement, E. Clipsham, J.P. Coad, I.H. Coffey[24], A. Colton, M. Comiskey[4], S. Conroy, M. Cooke, S. Cooper, J.G. Cordey, W. Core, G. Corrigan, S. Corti, A.E. Costley, G. Cottrell, M. Cox[7], P. Crawley, O. Da Costa, N. Davies, S.J. Davies[7], H. de Blank, H. de Esch, L. de Kock, E. Deksnis, N. Deliyanakus, G.B. Denne-Hinnov, G. Deschamps, W.J. Dickson[19], K.J. Dietz, A. Dines, S.L. Dmitrenko, M. Dmitrieva[25], J. Dobbing, N. Dolgetta, S.E. Dorling, P.G. Doyle, D.F. Düchs, H. Duquenoy, A. Edwards, J. Ehrenberg, A. Ekedahl, T. Elevant[11], S.K. Erents[7], L.G. Eriksson, H. Fajemirokun[12], H. Falter, J. Freiling[15], C. Froger, P. Froissard, K. Fullard, M. Gadeberg, A. Galetsas, L. Galbiati, D. Gambier, M. Garribba, P. Gaze, R. Giannella, A. Gibson, R.D. Gill, A. Girard, A. Gondhalekar, D. Goodall[7], C. Gormezano, N.A. Gottardi, C. Gowers, B.J. Green, R. Haange, A. Haigh, C.J. Hancock, P.J. Harbour, N.C. Hawkes[7], N.P. Hawkes[1], P. Haynes[7], J.L. Hemmerich, T. Hender[7], J. Hoekzema, L. Horton, J. How, P.J. Howarth[5], M. Huart, T.P. Hughes[4], M. Huguet, F. Hurd, K. Ida[18], B. Ingram, M. Irving, J. Jacquinot, H. Jaeckel, J.F. Jaeger, G. Janeschitz, Z. Jankowicz[22], O.N. Jarvis, F. Jensen, E.M. Jones, L.P.D.F. Jones, T.T.C. Jones, J-F. Junger, F. Junique, A. Kaye, B.E. Keen, M. Keilhacker, W. Kerner, N.J. Kidd, R. Konig, A. Konstantellos, P. Kupschus, R. Lässer, J.R. Last, B. Laundy, L. Lauro-Taroni, K. Lawson[7], M. Lennholm, J.Lingertat[13], R.N. Litunovski, A. Loarte, R. Lobel, P. Lomas, M. Loughlin, C. Lowry, A.C. Maas[15], B. Macklin, C.F. Maggi[16], G. Magyar, V. Marchese, F. Marcus, J. Mart, D. Martin, E. Martin, R. Martin-Solis[8], P. Massmann, G. Matthews, H. McBryan, G. McCracken[7], P. Meriguet, P. Miele, S.F. Mills, P. Millward, E. Minardi[16], R. Mohanti[17], P.L. Mondino, A. Montvai[3], P. Morgan, H. Morsi, G. Murphy, F. Nave[27], S. Neudatchin[23], G. Newbert, M. Newman, P. Nielsen, P. Noll, W. Obert, D. O'Brien, J. O'Rourke, R. Ostrom, M. Ottaviani, S. Papastergiou, D. Pasini, B. Patel, A. Peacock, N. Peacock[7], R.J.M. Pearce, D. Pearson[12], J.F. Peng[26], R. Pepe de Silva, G. Perinic, C. Perry, M.A. Pick, J. Plancoulaine, J-P. Poffé, R. Pohlchen, F. Porcelli, L. Porte[19], R. Prentice, S. Puppin, S. Putvinskii[23], G. Radford[9], T. Raimondi, M.C. Ramos de Andrade, M. Rapisarda[29], P-H. Rebut, R. Reichle, S. Richards, E. Righi, F. Rimini, A. Rolfe, R.T. Ross, L. Rossi, R. Russ, H.C. Sack, G. Sadler, G. Saibene, J.L. Salanave, G. Sanazzaro, A. Santagiustina, R. Sartori, C. Sborchia, P. Schild, M. Schmid, G. Schmidt[6], H. Schroepf, B. Schunke, S.M. Scott, A. Sibley, R. Simonini, A.C.C. Sips, P. Smeulders, R. Smith, M. Stamp, P. Stangeby[20], D.F. Start, C.A. Steed, D. Stork, P.E. Stott, P. Stubberfield, D. Summers, H. Summers[19], L. Svensson, J.A. Tagle[21], A. Tanga, A. Taroni, C. Terella, A. Tesini, P.R. Thomas, E. Thompson, K. Thomsen, P. Trevalion, B. Tubbing, F. Tibone, H. van der Beken, G. Vlases, M. von Hellermann, T. Wade, C. Walker, D. Ward, M.L. Watkins, M.J. Watson, S. Weber[10], J. Wesson, T.J. Wijnands, J. Wilks, D. Wilson, T. Winkel, R. Wolf, D. Wong, C. Woodward, M. Wykes, I.D. Young, L. Zannelli, A. Zolfaghari[28], G. Zullo, W. Zwingmann.

PERMANENT ADDRESSES

1. UKAEA, Harwell, Didcot, Oxon, UK.
2. University of Leicester, Leicester, UK.
3. Central Research Institute for Physics, Budapest, Hungary.
4. University of Essex, Colchester, UK.
5. University of Birmingham, Birmingham, UK.
6. Princeton Plasma Physics Laboratory, New Jersey, USA.
7. UKAEA Culham Laboratory, Abingdon, Oxon, UK.
8. Universidad Complutense de Madrid, Spain.
9. Institute of Mathematics, University of Oxford, UK.
10. Freien Universität, Berlin, F.R.G.
11. Royal Institute of Technology, Stockholm, Sweden.
12. Imperial College, University of London, UK.
13. Max Planck Institut für Plasmaphysik, Garching, FRG.
14. Risø National Laboratory, Denmark.
15. FOM Instituut voor Plasmafysica, Nieuwegein, The Netherlands.
16. Dipartimento di Fisica, University of Milan, Milano, Italy.
17. North Carolina State University, Raleigh, NC, USA
18. National Institute for Fusion Science, Nagoya, Japan.
19. University of Strathclyde, 107 Rottenrow, Glasgow, UK.
20. Institute for Aerospace Studies, University of Toronto, Ontario, Canada.
21. CIEMAT, Madrid, Spain.
22. Institute for Nuclear Studies, Otwock-Swierk, Poland.
23. Kurchatov Institute of Atomic Energy, Moscow, USSR
24. Queens University, Belfast, UK.
25. Keldysh Institute of Applied Mathematics, Moscow, USSR.
26. Institute of Plasma Physics, Academica Sinica, Hefei, P. R. China.
27. LNETI, Savacem, Portugal.
28. Plasma Fusion Center, M.I.T., Boston, USA.
29. ENEA, Frascati, Italy.

At 1st July, 1992